Neuropsychopharmacology (2007) 32, 1–16
© 2007 Nature Publishing Group All rights reserved 0893-133X/07 $30.00
www.neuropsychopharmacology.org

SSR180711, a Novel Selective α7 Nicotinic Receptor Partial Agonist: (1) Binding and Functional Profile

Bruno Biton*,[1], Olivier E Bergis[1], Frédéric Galli[1], Alain Nedelec[1], Alistair W Lochead[1], Samir Jegham[1], Danielle Godet[1], Christophe Lanneau[1], Raphaël Santamaria[1], Françoise Chesney[1], Jacques Léonardon[1], Patrick Granger[1], Marc W Debono[2], Georg A Bohme[2], Frédéric Sgard[3], François Besnard[3], David Graham[3], Annick Coste[1], André Oblin[1], Olivier Curet[1], Xavier Vigé[1], Corinne Voltz[1], Liliane Rouquier[1], Josiane Souilhac[4], Vincent Santucci[4], Christiane Gueudet[4], Dominique Françon[1], Régis Steinberg[4], Guy Griebel[1], Florence Oury-Donat[4], Pascal George[1], Patrick Avenet[1] and Bernard Scatton[1]

[1]Central Nervous System Research Department, Sanofi-Aventis, Bagneux, France; [2]Central Nervous System Research Department, Neurological Diseases, Sanofi-Aventis, Vitry sur Seine, France; [3]Functional and Molecular Biology Department, Sanofi-Aventis, Rueil Malmaison, France; [4]Central Nervous System Research Department, Sanofi-Aventis, Montpellier, France

In this paper, we report on the pharmacological and functional profile of SSR180711 (1,4-Diazabicyclo[3.2.2]nonane-4-carboxylic acid, 4-bromophenyl ester), a new selective α7 acetylcholine nicotinic receptor (n-AChRs) partial agonist. SSR180711 displays high affinity for rat and human α7 n-AChRs (K_i of 22 ± 4 and 14 ± 1 nM, respectively). *Ex vivo* ^{3}[H]α-bungarotoxin binding experiments demonstrate that SSR180711 rapidly penetrates into the brain (ID_{50} = 8 mg/kg p.o.). In functional studies performed with human α7 n-AChRs expressed in *Xenopus* oocytes or GH4C1 cells, the compound shows partial agonist effects (intrinsic activity = 51 and 36%, EC_{50} = 4.4 and 0.9 μM, respectively). In rat cultured hippocampal neurons, SSR180711 induced large GABA-mediated inhibitory postsynaptic currents and small α-bungarotoxin sensitive currents through the activation of presynaptic and somato-dendritic α7 n-AChRs, respectively. In mouse hippocampal slices, the compound increased the amplitude of both glutamatergic (EPSCs) and GABAergic (IPSCs) postsynaptic currents evoked in CA1 pyramidal cells. In rat and mouse hippocampal slices, a concentration of 0.3 μM of SSR180711 increased long-term potentiation (LTP) in the CA1 field. Null mutation of the α7 n-AChR gene totally abolished SSR180711-induced modulation of EPSCs, IPSCs and LTP in mice. Intravenous administration of SSR180711 strongly increased the firing rate of single ventral pallidum neurons, extracellularly recorded in anesthetized rats. In microdialysis experiments, administration of the compound (3–10 mg/kg i.p.) dose-dependently increased extracellular acetylcholine (ACh) levels in the hippocampus and prefrontal cortex of freely moving rats. Together, these results demonstrate that SSR180711 is a selective and partial agonist at human, rat and mouse α7 n-AChRs, increasing glutamatergic neurotransmission, ACh release and LTP in the hippocampus.
Neuropsychopharmacology (2007) **32,** 1–16. doi:10.1038/sj.npp.1301189; published online 4 October 2006

Keywords: nicotinic acetylcholine receptors; hippocampal slices; acetylcholine; long-term potentiation; ventral pallidum; SSR180711

INTRODUCTION

Nicotinic acetylcholine receptors (n-AChRs) are abundantly expressed in the central nervous system (CNS) and formed of various combinations of α (2–10) and β (2–4) subunits leading to pentameric homomeric or heteromeric channels, gated by acetylcholine (ACh). Among the large number of n-AChRs subtypes present in the CNS, α7 and heteromeric α4β2 n-AChRs are predominant (Tribollet *et al*, 2004). Although there is strong evidence that native α7 n-AChRs are homopentamers, some recent data suggest that rat α7 and β2 subunits can form functional heteromeric receptors (Khiroug *et al*, 2002). In addition, an homomeric α7 n-AChR variant called α7-2 has been described to be expressed in some peripheral and central neurons, displaying α-BTX sensitivity and an slower rate of desensitization (Severance and Cuevas, 2004).

In the hippocampus, a structure extensively studied for its involvement in learning and memory, α7 n-AChRs are densely expressed in both interneurons and glutamatergic pyramidal neurons. They are located presynaptically on nerve terminals and postsynaptically on dendritic spines and soma, where they modulate neurotransmitter release and are responsible for direct fast excitatory transmission, respectively (Fabian-Fine *et al*, 2001; Marchi *et al*, 2002;

*Correspondence: Dr B Biton, CNS Research Department, Sanofi-Aventis, 31 avenue Paul Vaillant-Couturier, 92220 Bagneux, France, Tel: +33 1 45 36 22 85, Fax: +33 1 45 36 29 09,
E-mail: bruno.biton@sanofi-aventis.com
Received 16 March 2006; revised 7 June 2006; accepted 20 June 2006
Online publication: 18 July 2006 at http://www.acnp.org/citations/Npp071806060171/default.pdf

Alkondon *et al*, 2000; Frazier *et al*, 1998). More recently, in two different neuronal preparations, α7 n-AChRs have been shown to be preferentially located at extrasynaptic site, activated by the spillover of ACh released at the active site (Jones and Wonnacott, 2004; Coggan *et al*, 2005). A large number of studies have demonstrated that α7 n-AChR stimulation can increase both glutamate and GABA release in a number of brain structures, including the hippocampus (Gray *et al*, 1996; Radcliffe *et al*, 1999; Reno *et al*, 2004). Furthermore, the activation of presynaptic α7 n-AChRs may trigger hippocampal ACh release from septal projections, consistent with the presence of α7 n-AChR mRNA in septo-hippocampal cholinergic neurons (Azam *et al*, 2003; Strong *et al*, 2003). Finally, long-term potentiation (LTP), an extensively used electrophysiological model of learning and memory formation, has been shown to be enhanced or even induced in the hippocampus after stimulation of α7 n-AChRs (Sawada *et al*, 1994; Hunter *et al*, 1994).

The α7 n-AChR subtype has recently been the focus of growing interest due to increasing evidence suggesting its involvement in psychiatric and neurological conditions such as schizophrenia and Alzheimer's disease (AD). Genetic studies suggest that the α7 n-AChR gene, located on chromosome 15, is linked to deficits in auditory and sensory gating in schizophrenic patients (De Luca *et al*, 2004a). Biochemical experiments have shown that high affinity α-bungarotoxin (α-BTX) binding sites (selectively overlapping with α7 n-AChRs in the brain) are decreased in the brain of patients suffering from schizophrenia or certain forms of dementia (Court *et al*, 1999, 2001; Perry *et al*, 2001; Freedman *et al*, 2001; De Luca *et al*, 2004b). It has also been suggested that in schizophrenic patients, who suffer from severe deficits in attention and have reduced learning capacities, α7 n-AChR-dependent cholinergic neurotransmission may be disrupted (Stip *et al*, 2005). The levels of α7 n-AChR proteins have been shown to be decreased in the brain of AD patients, a pathology characterized by severe memory impairments (Nordberg, 2001). In addition, a direct interaction of the β-amyloid peptide with α7 n-AChRs has also been described at native and recombinant rat α7 n-AChRs, leading to functional alteration of these receptors (Dineley *et al*, 2002; Grassi *et al*, 2003; Dougherty *et al*, 2003; Nordberg, 2001). It has been hypothesized that the attention and cognitive symptoms that are characteristic of schizophrenia and AD may involve a degeneration or a hypofunction of the cholinergic inputs, originating from the septum to the hippocampus (Grassi *et al*, 2003; Gray *et al*, 1996; Freedman *et al*, 2000). In support of this hypothesis, nicotine has been shown to significantly improve cognitive performance in AD or schizophrenic patients as well as in animal models of cognitive deficits (Rezvani and Levin, 2001). It is also noteworthy that the most commonly prescribed drugs for AD are acetylcholinesterase inhibitors, which increase cholinergic neurotransmission. Among these drugs, galantamine has also been shown to directly modulate n-AChRs. *In vitro* studies have shown that its protective effects *vs* β-amyloid toxicity were partially blocked by α-BTX, suggesting the involvement of α7 n-AChR receptors (Kihara *et al*, 2004). In addition, the stimulation of glutamate release via an action at presynaptic α7 and α4β2 n-AChRs has been suggested to be involved in the promnesic properties of nootropic drugs such as nefiracetam (Nishizaki *et al*, 2000). Therefore, the α7 n-AChR constitutes an attractive potential drug target for diseases associated with a deficit in cholinergic or glutamatergic transmission, including schizophrenia and AD.

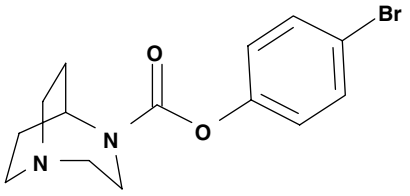

Figure 1 Chemical structure of SSR180711 (1,4-Diazabicyclo[3.2.2]nonane-4-carboxylic acid, 4-bromophenyl ester).

Herein, we report on the binding profile and *in vitro*/*vivo* functional properties of a novel α7 n-AChR partial agonist, SSR180711 (1,4-Diazabicyclo[3.2.2]nonane-4-carboxylic acid, 4-bromophenyl ester) (Figure 1). The pharmacological profile of SSR180711 in experimental models predictive of therapeutic activity on cognitive symptoms of schizophrenia is presented in a companion article (Pichat *et al*, 2006).

MATERIALS AND METHODS

Drugs

SSR180711 was synthesised by the Medicinal Chemistry Department of Sanofi-Aventis (Bagneux, France). (−)Nicotine (tartrate salt), cytisine, mecamylamine, methotrexate, methyllycaconitine (MLA), α-bungarotoxin, bicuculline and (+)-MK-801 were purchased from Sigma-Aldrich (Saint Quentin Fallavier, France). Cyprofloxacin was purchased from Euromedex. All other compounds for cell cultures were obtained from Invitrogen (Cergy, France). [^{3}H]-cytisine (32 C_i/mmol) was purchased from NEN Life Science Products (Paris, France). [^{3}H]-α-bungarotoxin (60 C_i/mmol) and [^{3}H]-epibatidine (55 C_i/mmol) were purchased from Amersham Biosciences (Orsay, France). NBQX (6-nitro-7-sulfamoylbenzo[f]quinoxaline-2,3-dione), 2-APV (D-2-amino-5-phosphonovaleric acid) and CGP52432 were purchased from Tocris (Ellesville, USA).

Animals

Experimental subjects were supplied by Iffa-Credo (Les Oncins, France) or Charles-River (St Aubin-les-Elbeuf, France), unless specified otherwise. Animals were kept in temperature- and humidity-controlled rooms (22°C, 50%) with lights on from 0700 to 1900 (except when indicated otherwise), with water and food available *ad libitum*. All experiments were performed in accordance with the 'Guide and Care and Use of Laboratory Animals' (National Institute of Health) and were approved by the in-house Animal Ethics Committee.

Mice for homozygous null mutation for α7 n-AChR gene were provided by the Baylor College of Medicine, (Houston, TX, USA). The mutation deletion concerns the last three exons (8–10) of the α7 locus (Orr-Urtreger *et al*, 1997).

Female *Xenopus laevis* were supplied by the CNRS (Montpellier, France).

Cell Lines

Cell lines stably expressing either human α7 or human α4β2 n-AChR, designed as hα7-GH_4C_1 and hα4β2-HEK293 respectively, were generated by the Molecular Genomic Department of Sanofi-Synthélabo Recherche (Rueil-Malmaison, France). For patch-clamp experiments, GH4C1 cells were transiently transfected with a pTracer expression vector containing the hα7 n-AChR cDNA (Molecular Genomic Department of Sanofi-Synthélabo Recherche, Rueil-Malmaison, France), using FuGene according to manufacturer's protocol. SH-SY5Y, and IMR32 cell lines, which have been shown to constitutively express the human α3β4 n-AChR subtype (Lukas, 1993; Nelson *et al*, 2001), and human medulloblastoma cells (TE671), which natively express the human α1β1γδ n-AChR subtype (Schoepfer *et al*, 1988) were purchased from ATCC (Biovalley, Marne La Vallée, France). HEK293 cells stably expressing the human α3β2 n-AChR subtype (hα3β2-HEK293) were supplied by Professor J Lindstrom (University of Pennsylvania, USA).

Cell lines were maintained as described by suppliers with some modifications. hα7-GH_4C_1 were grown in Nutrient Mixture F10-Ham buffer supplemented with 10% horse serum, 2.5% fetal bovine serum, 500 U/ml penicillin, 500 μg/ml streptomycin and 100 μg/ml zeocin. hα4β2-HEK293 were maintained in Modified Eagle Medium (MEM) supplemented with 10% dialyzed fetal bovine serum, 500 U/ml penicillin, 500 μg/ml streptomycin, 500 μg/ml geneticin, 20 μM mecamylamine, 100 nM methotrexate, and 10 μg/ml cyprofloxacin. At 1 day before collection, cells were placed in mecamylamine free medium culture. SH-SY5Y cells were grown in Ham's F12/MEM (v/v) supplemented with 10% fetal bovine serum, 1% antibiotics (penicillin, streptomycin) and 1% non-essential amino acids. Except for hα7-GH_4C_1, nicotine (100 μM–1 mM) was added into the culture medium and the cells were incubated for 24–48 h before harvesting in order to upregulate n-AChR expression (Wang *et al*, 1998). All cell lines were grown at 37°C in a humidified atmosphere containing 5% CO_2.

For pellets generation, the cell monolayers were washed once with phosphate buffered saline, scrapped and centrifuged (300*g*, 5 min). Pellets were stored at −80°C until binding studies. For patch-clamp experiments, cells were seeded on glass coverslips (2×10^5 cells/coverslip) and placed in 12-wells Corning dishes and incubated at 37°C in a humidified atmosphere containing 5% CO_2/95% air for 1–3 days before use.

Cultured Hippocampal Neurons

Briefly, the brains of 1-day newborn Sprague–Dawley rats were removed and their hippocampi isolated and sliced in 1 mm cubes. Hippocampal cubes were trypsinized and the cells were dissociated by gentle trituration. Cells were resuspended in basal Eagle's culture medium containing 10% fetal bovine serum, 25 mM KCl, 2 mM glutamine, 100 mg/ml gentamicin, then seeded on laminin-coated glass coverslips (0.25×10^6 cells/coverslip), and placed in 12-well Corning dishes. Cells were incubated at 37°C in a humidified atmosphere containing 5% CO_2/95% air. Cytosine β-D-arabinoside (1 mM) was added 48 h after seeding to prevent the proliferation of non-neuronal cells. Neurons were cultured at least 10 days before patch-clamp experiments.

Acute Hippocampal Slices

Coronal brain slices including hippocampi (0.3 mm thick) were prepared from wild-type or homozygous α7 n-AChR gene knock-out C57bl6/j mice (P17-P25). Briefly, animals were killed and their brains were removed and sectioned on a Leica vibroslicer VT1000S in artificial cerebrospinal fluid (aCSF) solution containing 126 mM NaCl, 3.5 mM KCl, 1 mM $MgCl_2$, 1.15 mM KH_2PO_4, 1 mM $CaCl_2$, 25 mM $NaHCO_3$, and 11 mM glucose, at approximately 0°C, aerated with 95% O_2, 5% CO_2 to a final pH of 7.35. The osmolarity of aCSF solution was 315 mosmo. The slices were maintained in an immerge-style chamber at room temperature in slice solution as already described (Lanneau *et al*, 2002). After at least 1 h, slices were transferred to the record chamber and perifused continuously with aCSF solution containing 1 μM of strychnine. The temperature was maintained at 30–32°C (TC 324B, Warner instruments corp., USA).

Rat transverse hippocampal slices (0.5 mm thick) were obtained from male Sprague–Dawley rats (150–220 g). Dissected hippocampi were sliced using a Mc Ilwain tissue chopper. After 1-h recovery at room temperature in oxygenated artificial cerebrospinal fluid (aCSF, see composition below), slices were transferred to an immerge-style recording chamber and perifused (2 ml min^{-1}) at 34–35°C.

aCSF composition (in mM): NaCl: 126, KCl: 3.5, NaH_2PO_4: 1.1, $MgCl_2$: 1.3, $CaCl_2$: 2, $NaHCO_3$: 25, Glucose: 11.

Membrane Preparations

Rat nicotinic receptors. For α7-nAChR-binding studies, rats (Sprague–Dawley, 180–220 g) were killed by decapitation and whole brain except cerebellum was removed and placed on ice. Tissues were homogenized at 4°C in 15 volumes of ice-cold buffer containing 20 mM HEPES, 118 mM NaCl, 4.8 mM KCl, 2.5 mM $CaCl_2$, 1.2 mM $MgCl_2$, 2 μg/ml aprotinin, 20 μM bestatin (pH 7.4) and the pellet was washed twice by centrifugation for 20 min at 4°C (40000*g*). The resulting pellet was stored at −80°C. The day of experiment, the pellet was homogenized in 20 ml of ice-cold binding buffer followed by a centrifugation at 40 000*g* as above.

Human nicotinic receptors. hα7-GH_4C_1 cell pellets were suspended in 15 ml of ice-cold HEPES buffer (composition described above for rat α7 n-AChR) and centrifuged for 20 min at 4°C (41 500*g*). hα4β2-HEK293 cell pellets were homogenized in ice-cold 50 mM Tris-HCl binding buffer (pH 7.4) containing 120 mM NaCl; 5 mM KCl; 2.5 mM $CaCl_2$, and 1 mM $MgCl_2$ and washed twice by centrifugation 15 min at 4°C (41 500*g*). hα3β2–HEK293 cells were homogenized in HEPES-binding buffer containing 140 mM NaCl, 1.5 mM KCl, 2 mM $CaCl_2$, 1 mM $MgSO_4$, 1 mM *p*-aminobenzamidine dihydrochloride and 25 mM HEPES (pH 7.5) and washed twice by centrifugation (45 000*g* for 15 min). The membrane preparation was incubated 15 min at 25°C with fresh buffer and centrifuged (45 000*g* for 15 min). A protocol similar to that used for hα3β2-HEK293 cells was followed for hα3β4

n-AChR expressed in SH-SY5Y cells (hα3β4-SH-SY5Y). For hα1 n-AChR, TE671 cell pellets were homogenized in 20 mM HEPES-binding buffer (pH 7.4) containing 118 mM NaCl, 4.8 mM KCl, 2.5 mM $CaCl_2$, 1.2 mM $MgCl_2$, 2 μg/ml aprotinin and 20 μM bestatin and washed twice by centrifugation for 15 min at 4°C (41 500*g*). The pellet was suspended in HEPES buffer, incubated at room temperature for 15 min and centrifuged once again as previously described.

Receptor Binding

Rat and human α7 n-AChRs. [3H]α-BTX binding was carried out as previously described with slight modifications (Marks *et al*, 1986; Quik *et al*, 1996). Samples containing either $h\alpha_7$-GH_4C_1 cell membranes (150–200 μg of protein) or rat brain membranes (100–200 μg of protein) and SSR180711 from 10^{-10} to 10^{-6} M were preincubated for 30 min at 37°C in HEPES-binding buffer (pH 7.4) supplemented with 0.1% BSA and then for 60 min with 1 nM [^{3}H]α-BTX ($K_d = 2.73$ and 2.71 nM for rat and human α7 n-AChRs, respectively) in the dark. Nonspecific binding was determined in the presence of 1 μM α-BTX.

Human α3β2 n-AChRs. [^{3}H]epibatidine binding was performed as previously described (Parker *et al*, 1998). Samples containing hα3β2-HEK293 cell membranes (2–10 μg of protein), 0.05 nM [3H]epibatidine ($K_d =$ 0.018 nM) and SSR180711 from 10^{-9} to 10^{-5} M were incubated in 25 mM HEPES-binding buffer (pH 7.5) for 2 h at 25°C (final volume: 1 ml). Nonspecific binding was determined in the presence of 100 μM (−)nicotine.

Human α3β4 n-AChRs. [^{3}H]epibatidine binding on SH-SY5Y cell membranes was performed as described for human α3β2 n-AChR binding except for radioligand concentration: 0.3 nM [^{3}H]epibatidine ($K_d = 0.17$ nM).

Human α4β2 n-AChRs. [^{3}H]-Cytisine binding was performed as previously described with slight modifications (Pabreza *et al*, 1991; Gopalakrishnan *et al*, 1996). Samples containing hα4β2-HEK293 cell membranes (1–10 μg of protein), the test compound and 0.5 nM [^{3}H]-cytisine ($K_d = 0.59$ nM) were incubated in 50 mM Tris-HCl binding buffer (pH 7.4) for 2 h at 4°C (final volume: 200 μl). Nonspecific binding was determined in the presence of 10 μM (−) nicotine.

Human α1β1γδ n-AChRs. [^{3}H]α-BTX binding was carried out as described previously (Lukas *et al*, 1979; Lukas, 1986). Samples containing TE671 cell membranes (100–150 μg of protein) and SSR180711 from 10^{-9} to 10^{-5} μM were incubated at 37°C in 20 mM HEPES-binding buffer (pH 7.4) supplemented with 0.1% BSA. After 15 min, 2 nM [^{3}H]α-BTX ($K_d = 4.93$ nM) were added and the incubation carried out for 2 h at 37°C in the dark (final volume: 250 μl). Nonspecific was determined in the presence of 1 μM α-BTX.

For all binding experiments, the incubations were stopped by rapid vacuum filtration over GF/C glass fiber filters for the α7 and α1β1γδ nAChR binding and over GF/B glass fiber filters for the α3β2, α4β2 and α3β4 nAChR binding. The radioactivity retained on the filters was counted by liquid scintillation spectrometry in the presence of 10 ml Ultima Gold (Packard).

Protein concentrations were determined according the method of Lowry (Lowry *et al*, 1951) using the Bio-Rad DC Protein Assay.

Data analysis. Data were evaluated by computer-assisted nonlinear regression analysis techniques and represented either as the drug concentration required to inhibit 50% of total specific binding (IC_{50}) or as inhibition constants (K_i). These latter were calculated from radioligand binding competition curves as $K_i = IC_{50}/(1 + ([L]/K_d))$, using the Cheng–Prusoff equation (Cheng and Prusoff, 1973), where [L] represents the radioligand concentration used and K_d its dissociation constant for the receptor under study.

Receptor Selectivity

Interaction of SSR180711 with 100 binding sites, including all major classes of neurotransmitter receptor, uptake systems, ion channels, and enzymes was examined (CEREP, Celle L'Evescault, France). SSR180711 was tested in all assays at 10 μM. Each determination was made in duplicate.

Ex Vivo Inhibition Studies

Ex vivo [^{3}H]α-BTX binding studies were performed according to the method previously described (Flesher *et al*, 1994). Male OF1 mice, weighing 20–25 g, were used. Animals were administered with SSR180711 or vehicle i.p. 30 min before or orally, 60 min before killing. For p.o. treatment, animals were deprived of food for 16 h before the experiment. Mice were killed by decapitation and cortical tissues were rapidly homogenized and incubated 1 h at 37°C with 2 nM of [^{3}H]α-BTX. Nonspecific [^{3}H]α-BTX binding was determined with 100 μM MLA. The reaction was stopped by a rapid filtration over Wathman GF/C glass filters. The radioactivity was quantified by liquid scintillation in counter. A time–course study was performed with administration of 10 mg/kg p.o. of SSR180711 using the protocol described above. [^{3}H]α-BTX binding was evaluated 5, 15, 30 min and 1, 2, and 4 h after treatment.

Statistical analysis. For time course study, Kruskal–Wallis test was used followed by multiple two-side comparison test *vs* time of control group with Bonferroni-Holm correction in case of significance of the global analyses (using SAS V8.2 via Everstat V5.0 interface).

Electrophysiological Studies

Voltage-clamp in Xenopus oocytes. Oocytes were harvested from female *Xenopus laevis* (150–300 g) as previously described (Canton *et al*, 2001), injected with 5 ng human α7 mRNA and maintained for at least 2 days at 16–17°C before being used for voltage-clamp experiments. Current responses were recorded in a small recording chamber superfused at approximately 3 ml/min with recording medium of the following composition: NaCl (115 mM), KCl (2.5 mM), $BaCl_2$ (2.4 mM), HEPES (10 mM), and atropine (1 μM). Membrane voltage was clamped at a holding

potential of −80 mV through 3 M KCl-filled glass microelectrodes. SSR180711 was prepared as a 10^{-2} M stock solution in dimethyl sulfoxide (DMSO). Appropriate final bath concentrations were obtained by dilution in the recording medium. Amplitude of agonist responses were normalized with respect to control responses elicited by a near half-maximally effective concentration of 300 μM ACh. Test drug applications were separated by 5 min washout periods and interleaved with control ACh applications. EC_{50} values were calculated on normalized data from five to seven oocytes, fitted according to a sigmoidal nonlinear least square regression procedure and given with their 95% confidence interval.

Patch-clamp in cultured cell lines and hippocampal neurons. Experimental chambers containing seeded coverslips, were placed on the stage of an inverted microscope (Olympus IMT2) equipped with Hoffman optics (Modulation Contrast, New York, NY) and the cells viewed at a total magnification of ×400. A gravity fed perfusion valve control system was used (VC-66CST, Warner-Lambert, USA) driven by Clampex (8.2 version) connected to a nine ways manifold ended by a glass tube (500 μm opening) placed at <1 mm of the recorded cells. In all experiments, a separate glass tube achieved ACh superfusion.

The whole-cell configuration of the patch-clamp technique at room temperature was used. The holding voltage was set at –60 mV. Pipettes were pulled from thick-walled borosilicate glass capillaries (Harvard Apparatus, Edenbridge, UK) on a horizontal two-stages puller (P97, Sutter Instruments, USA) and had a resistance of 5–10 mΩ when filled with the pipette solution (see below). Pipettes were brought into contact with the cells with a three-dimensional piezoelectric micromanipulator (Burleigh PCS1000, Dipsi Industrie, Chatillon, France). Whole-cell currents were recorded with an Axopatch 1D (Axon Instruments, Burlingame, CA) driven by Clampex software (8.2 version, Axon Instrument, Foster City, USA).

The standard extracellular solution contained (in mM): NaCl (147), KCl (5), $CaCl_2$ (2), $MgCl_2$ (1), HEPES (10). pH was set to 7.4 with TrisOH 1 M. The pipette was filled with an intracellular pipette medium, containing (in mM): CsCl (140), $MgCl_2$ (1), $CaCl_2$ (1), EGTA (11), ATP (4), and HEPES (10) and the pH was set to 7.2 with TrisOH (1 M). Drugs were diluted in purified water or DMSO whose concentration did not exceed 0.08% in the final solutions used.

Electrophysiological responses were quantified by calculating the mean current amplitudes induced by the drugs relative to ACh induced-current amplitudes. Concentration–dependence curve calculations used the least square fitting routine of the 'Origin^{TM}' software (Microcal Software, Southampton). These curves were fitted by using the single site equation: $y = \text{Max}^{*}C^n/(C^n + EC_{50}^n)$ where C is the concentration of the tested compound, n the Hill coefficient and Max the maximal effect. Parameters providing the best fit are given with a 95% confidence interval.

hα3β2, hα3β4, and hα1β1γδ n-AChR-mediated currents in HEK293, IMR-32, and TE671 cell lines, respectively.

The effects of SSR180711 at 100 μM were compared to those of ACh applied at 1 mM (IMR-32 and α3β2n-AChRs expressed by HEK cells), or 100 μM (α1β1γδ n-AChRs expressed in TE671 cells), concentrations that produced maximal responses.

hα7 n-AChR-mediated currents in GH4C1 cells. GFP expressing/fluorescent cells were identified under UV illumination and then recorded under the whole-cell configuration of the patch-clamp technique at a holding voltage of −60 mV. Maximal effect of SSR180711 and reference compounds were assessed by comparison with the effect of 1 mM of ACh, a concentration inducing currents of maximal amplitudes. In order to evaluate the desensitization of α7 n-AChRs each studied concentration of SSR180711 or reference compound was preceded by two—and followed by three—applications of ACh at 1 mM (superfusion duration: 7 s, 1 min interval between each).

rα7 n-AChR-mediated currents in cultured hippocampal neurons. Presynaptic and somatodenditic α7 n-AChR-mediated currents were recorded by application of SSR180711 in the absence or the presence of 0.2 μM of tetrodotoxin, respectively, and identified by their sensitivity to α-BTX. Electrophysiological responses were quantified by calculating the mean current amplitudes induced by the drugs. Concentration–dependence curve calculations used the least square fitting routine of the 'OriginTM' software (Microcal Software, Southampton). These curves were fitted by using the single site equation: $y = \text{Max}^{*}C^n/(C^n + EC_{50}^n)$ where C is the concentration of the tested compound, n the Hill coefficient and Max the maximal effect. Parameters providing the best fit are given with a 95% confidence interval.

Patch-clamp in mouse acute hippocampal slices. Electrical recordings were made from CA1 pyramidal cell somata in slices under visual control with a ×10 water-immersion lens on an upright microscope (BX50WI; Olympus Optical, Tokyo, Japan), using patch pipettes made of borosilicate glass (resistance, 5–10 MΩ). Pipettes were filled with 135 mM K gluconate, 8 mM NaCl, 2 mM $MgCl_2$, 10 mM HEPES, 2 mM Mg ATP, 0.3 mM Na GTP, 5 mM Na QX-314. The pH was adjusted at 7.2 with KOH. Capacitance was fully compensated by a patch-clamp amplifier (Axopatch 1D; Axon Instruments, Foster City, CA). Cells were identified as pyramidal neurons according to both electrical and anatomical criteria. To elicit excitatory post-synaptic currents (eEPSCs), concentric bipolar stimulation electrode (platinium/iridium, 12.5 μm i.d., FHC, MA) connected to a DS3 isolated stimulator (Digitimer, USA) was placed on the pyramidal layer of CA1. Paired-pulse protocol (50 ms interval, F = 0.2 Hz) was used to generate eEPSCs, with holding potential set at −70 mV and the bath solution supplemented with 1 μM bicuculline methiodide. For inhibitory post-synaptic current (IPSC) recording, the stimulation electrode was placed in the stratum radiatum and IPSCs were evoked using a paired-pulse protocol (70 ms interval, F = 0.03 Hz). The holding potential of CA1 pyramidal neurons was held at −30 mV, bath solution supplemented with 2-APV, NBQX and CGP52432 to inhibit NMDA, AMPA/KA, and GABA(B) receptors, respectively.

LTP in acute hippocampal slices (rat and mouse). Bipolar electrodes were placed on the Schaeffer-collateral fibers to

stimulate (0.03 Hz) the CA1 region. Excitatory postsynaptic potentials (EPSPs) were recorded with glass microelectrodes filled with NaCl 2 M. The amplitudes of EPSPs were measured on-line with Analysis of Neuronal Responses (ARN) software (Notocord, Croissy sur Seine, France). Two trains (700 ms) of high frequency stimulation (HFS—100 Hz) were applied with a 30 s delay to induce LTP. Drugs were applied 10 min before and washed out 30 min after HFS. Data were collected every 30 s and analyzed every 5 min by a two-ways ANOVA. Subsequent comparisons between test groups and controls were carried out using Dunnett's *t*-test.

Electrophysiological recordings in the ventral pallidum of anesthetized rats. Experiments were carried out in male Sprague–Dawley rats, weighing 280–400 g. Animals were anesthetized with chloral hydrate (400 mg/kg intreperitoneal (i.p.)) and placed in a Mod. 900 stereotaxic apparatus (David-Kopf Instruments). The lateral tail vein was catheterized to allow slow infusion of chloral hydrate (120 mg/kg/h) using a micro-infusion pump (Harvard, Edenbridge, UK). A 3-way stopcock on the pump circuit was used for intravenous bolus injections of drugs. The animal was maintained at $37 \pm 0.1^{\circ}$C using a temperature-controlled heating pad (Harvard).

The scalp and underlying tissues were resected and 2×2 mm burr holes were drilled into the skull above the ventral pallidum (VP), according to the stereotaxic coordinates of Paxinos and Watson's (1998) atlas. Analgesia of the wounds and pressure points was ensured by initial 5% lidocaïne hydrochloride spray (Xylocaïne®, Astra-Zeneca).

Pulled (Narishige PE-2 puller, Tokyo, Japan) glass, 1 μm-tipped micropipettes were filled with 1 M NaCl or 0.5 M sodium acetate containing 2% Pontamine sky blue (impedance 5–10 MΩ at 100 Hz). They were lowered to the vicinity of VP cells (0.4 mm posterior to bregma, 1.9–2.2 mm lateral to the midline, depth 7.5–8.5 mm from the cortical surface) using a MMO-203 hydraulic microdrive (Narishige, Tokyo, Japan). Action potentials (spikes) were amplified with a DAM80 AC amplifier (WPI, Sarasota, Fl, USA), filtered (bandpass 400–4000 Hz) and monitored on both a digital oscilloscope and an audio amplifier. A window discriminator simultaneously transmitted the transformed signals to a micro1401 intelligent laboratory interface (Cambridge Electronic Design, CED, Cambridge, UK) connected to a PC. Firing rate time histograms were generated on-line and processed using 'Spike2' software (CED).

Once a cell was detected, its firing rate was allowed to stabilize for 5–10 min before drug injection and recording was then continued onward. In interaction experiments, MK-801 or MLA were administered 15 or 30 min after SSR180711, respectively. All drugs were injected i.v. in distilled water solutions (1 ml/kg v/w).

The mean firing rate (in spikes/s) was calculated over 5-min periods. In the SSR180711 *per se* experiments, each of the consecutive mean rate values following drug (or vehicle) administration was compared to its 5-min predrug (or prevehicle) counterpart. In interaction experiments, comparison were made between each of the consecutive rate values following, and that preceding, MLA or MK-801 administration.

As the animals were their own controls, the statistical significance of post- predrug differences was assessed using paired ANOVA followed by Duncan's multiple comparison test.

Microdialysis Studies and Biochemical Analysis of Extracellular Levels of ACh in the Hippocampus and Prefrontal Cortex of Freely Moving Rats

Adult male Sprague–Dawley rats (250–330 g) were anesthetized with chloral hydrate (400 mg/kg, i.p.), placed in a stereotaxic frame (David Kop Instruments, Tujunga, CA, USA) and implanted with a guide cannula above the ventral hippocampus (5.0 mm posterior and 5.0 mm lateral to bregma) or above the medial prefrontal cortex (3.2 mm anterior and 0.8 mm lateral to bregma). After recovery (2 days), a microdialysis probe (CMA 12, length 4 mm and outer diameter 0.5 mm, Carnegie Medicine, Stockholm, Sweden), was positioned within the guide cannula (vertical coordinates: 7 mm and 5 mm under the dura mater, for hippocampus and prefrontal cortex, respectively) and perfused at a constant flow rate of 2 μl/min with artificial cerebrospinal fluid containing 0.3 μM of neostigmine to reduce ACh degradation in the dialysate. The animals were left for at least 3 h to allow the system to equilibrate, then dialysate samples were collected every 20 min and ACh levels were measured using HPLC with electrochemical detection as previously described (Steinberg *et al*, 1995).

The average concentration of four stable fractions immediately preceding i.p. or p.o. administration of SSR180711 or vehicle was defined as the 100% control value and acetycholine levels in serial perfusates were converted to a percentage of this mean value. Statistical analysis was carried out by a two-way ANOVA (with time as the within factor, and treatment as the between factor), followed by one-way ANOVA's at each time, with Dunnett's *post hoc* tests. On completion of the microdialysis experiments, the animals were sacrificed and their brains were removed and sliced to confirm probe placement.

RESULTS

Radioligand Binding Studies

In vitro binding experiments. SSR180711 displaced specific [^{3}H]α-BTX binding to the rat and human α7 n-AChRs with K_i values of 22 ± 4 or 14 ± 1 nM, respectively ($n = 4$). The corresponding IC_{50} values were 30 ± 5 and 18 ± 1 nM, respectively. This compound was selective for the α7 receptor subtype compared to α4β2, α3β2, α3β4, and α1β1γδ human n-AChR subtypes ($IC_{50} > 5$ μM; Table 1). Furthermore, SSR180711 was studied at 10 μM in a 100 standard receptor binding profile (CEREP) and found to be devoid of activity (inhibition lower than 50%) for the ionic channels, neurotransmitter, or peptide receptors tested (data not shown).

In Vitro Functional Characterization

Recombinant hα7 n-AChRs transiently expressed in Xenopus *oocytes.* Application of SSR180711 elicited typical concentration-dependent inward currents (Figure 2a).

Compared to ACh, SSR180711 behaved as a potent, partial agonist. The EC_{50} value for SSR180711 was 4.4 μM (2.5–7.8 μM) and the E_{max} value reached 51% of the response to a maximally active concentration of 3 mM ACh (Figure 2b). The latter exhibited an EC_{50} value of 411 μM (223–757 μM) in this experimental series.

Table 1 IC_{50} Values of SSR180711 at Different Subtypes of Rat and Human n-AChRs

n-AChR subtypes	SSR180711 IC_{50} (nM)
rα7	30 ± 5
hα7	18 ± 1
hα4β2	> 10 000
hα3β2	#5000
hα3β4	> 10 000
hα1β1γδ	> 10 000

Recombinant hα7 n-AChRs transiently expressed in GH4C1 cells. When measuring peak current amplitude, SSR180711 behaved as a partial agonist with an intrinsic activity (IA) of 36% *vs* ACh (1mM) and an EC_{50} value of 0.9 μM (0.6–1.4 μM, $P = 0.05$) (Figure 2c and d). Even at the high concentration of 10 μM, SSR180711 only induced a short-lasting desensitization of hα7 n-AChRs, as characterized by the rapid recovery of ACh-induced currents after 1-min drug washout (Figure 2c). Under the same experimental conditions, nicotine was also found to be a partial agonist with an IA of 58% and an EC_{50} value of 18 μM (13–28 μM, $P = 0.05$) (Figure 2d). ACh was characterized

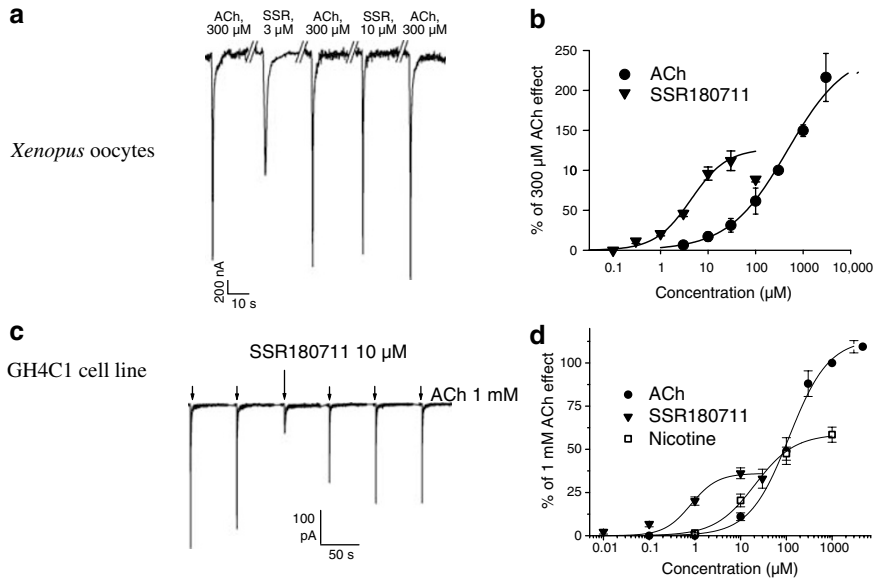

Figure 2 SSR180711 is a potent partial agonist at human α7 n-AChRs expressed in *Xenopus* oocytes or GH4C1 cells. (a and b) hα7 n-AChRs expressed in *Xenopus* oocytes. (a) Examples of currents elicited by application of a near half-maximal concentration of ACh (300 μM) in alternation with the indicated concentration of SSR180711. Traces are consecutive acquisitions separated by 5 min. (b) Concentration–response relationship for peak amplitudes of inward currents induced by ACh or SSR180711 normalized with respect to 300 μM ACh. Data are mean ± SEM from five to seven oocytes. (c and d) hα7 n-AChRs expressed in GH4C1 cells. (c) Typical recording, showing the fast inward current induced by the superfusion of 10 μM of SSR180711 and the fast recovery of the following ACh-induced currents. SSR180711 action was preceded by two—and followed by three—applications of ACh at 1 mM (superfusion duration: 7 s, 1 min interval between each). (d) Concentration–response curves for ACh (circle), nicotine (square) and SSR180711 (triangle). For each agonist, data points indicate the mean ± SEM of current amplitudes ($n = 2$–14 cells), normalized to 1 mM of Ach-induced current. Curves are the best fit of data point with the following single site equation: $y = \text{Max}*C^n/(C^n + EC_{50}^n)$, where C is the concentration, Max the maximal effect, and n the hill coefficient.

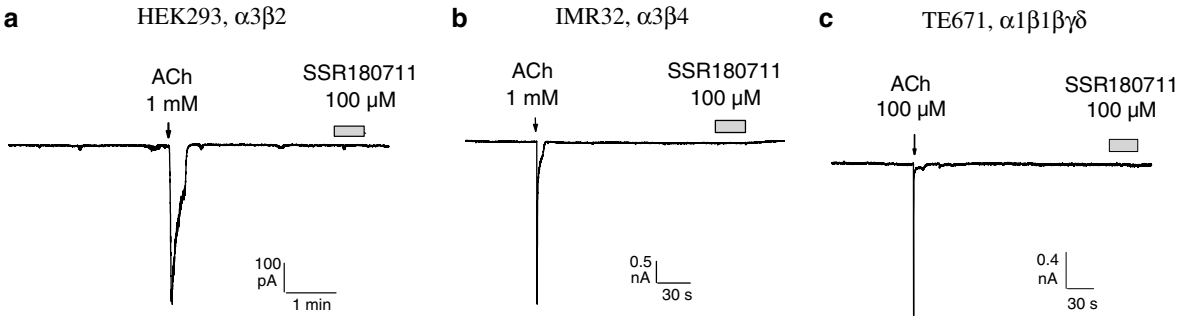

Figure 3 SSR180711 functional selectivity profile at other human n-AChRs. Typical patch-clamp recordings showing the variation of steady-state current as a function of time (holding potential = −60 mV). SSR180711 applied at 100 μM was ineffective at hα3β2 n-AChRs stably expressed in HEK293, α3β4 n-AChRs natively expressed in IMR32 cell line and at hα1β1γδ n-AChRs natively expressed in the TE671 cell line. ACh (1 mM or 100 μM) was used as reference and elicited in the same cells inward currents with time courses characteristic of the studied subtype.

as a full agonist with an EC_{50} value of 75 μM (44–126 μM, $P = 0.05$).

Functional selectivity profile at different human n-AChR subtypes. In addition to binding studies, the selectivity of SSR180711 at other human n-AChRs, which are known to play a role in nicotine side effects, has been assessed by using the whole cell configuration of the patch-clamp technique. SSR180711 at 100 μM was found to be ineffective at hα1β1γδ n-AChRs natively expressed in the TE671 cell line, at hα3β2 n-AChRs stably expressed in hα3β2-HEK293 and at hα3β4 n-AChRs natively expressed in the IMR32 cell (Figure 3a, b and c).

Effect at native rat α7 n-AChRs expressed in cultured hippocampal neurons. When applied at 1 μM on pyramidal-like neurons voltage-clamped at −60 mV (Figure 4a), SSR180711 generally induced fast, large, and repetitive inward currents (see inset Figure 4b) which were blocked by α-BTX, bicuculline, and tetrodotoxin (TTX), suggesting that these currents result from stimulated GABA release via activation of presynaptic α7 n-AChRs (Figure 4b, c and d). However, in about one third of the recorded neurons, SSR180711 also induced small inward currents, which were still blocked by α-BTX but not affected by bicuculline and almost insensitive to TTX (Figure 5a, b and c). These currents were most likely attributed to the direct activa-

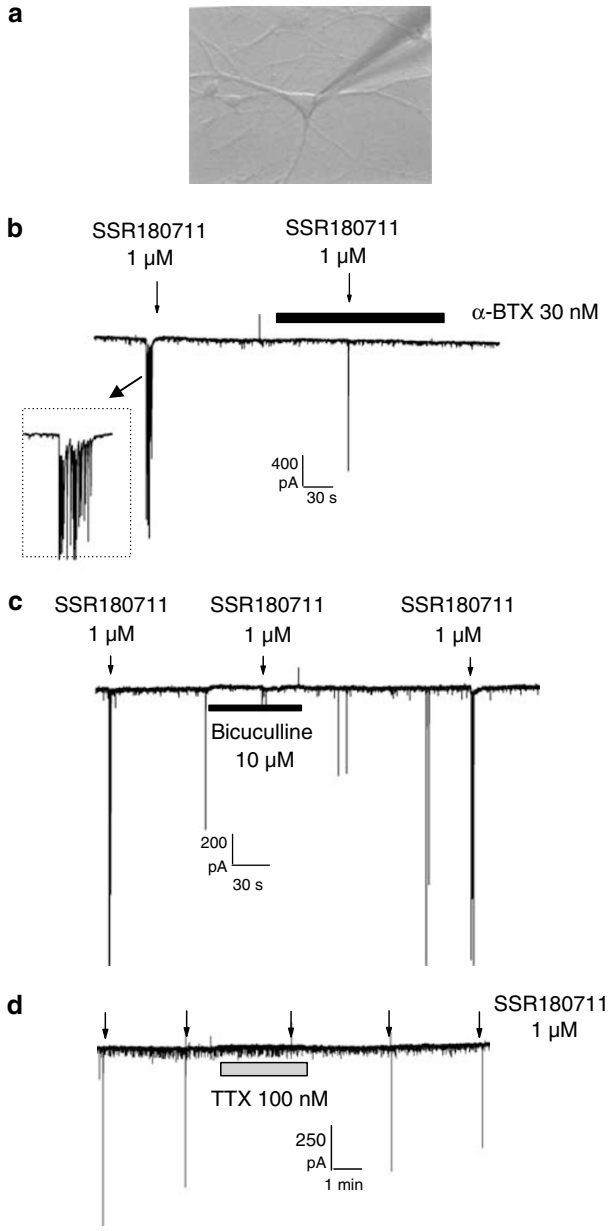

Figure 4 Effect of SSR180711 at rat native presynaptic α7 n-AChRs expressed in cultured hippocampal neurons. (a) Picture showing a characteristic pyramidal neuron, the patch pipette and the well-developed neuronal network in cultured hippocampal neurons. (b) Original trace showing the variation of the steady-state current as a function of time at a holding potential of −60 mV. SSR180711 at 1 μM induced large, fast, and repetitive inward currents (the inset shows the current time-course at an expanded time scale). Preapplication of α-BTX completely blocked SSR180711-induced current. In the same conditions described in (a), SSR180711-induced currents were completely blocked by 10 μM of bicuculline (c) or 100 nM of TTX (d).

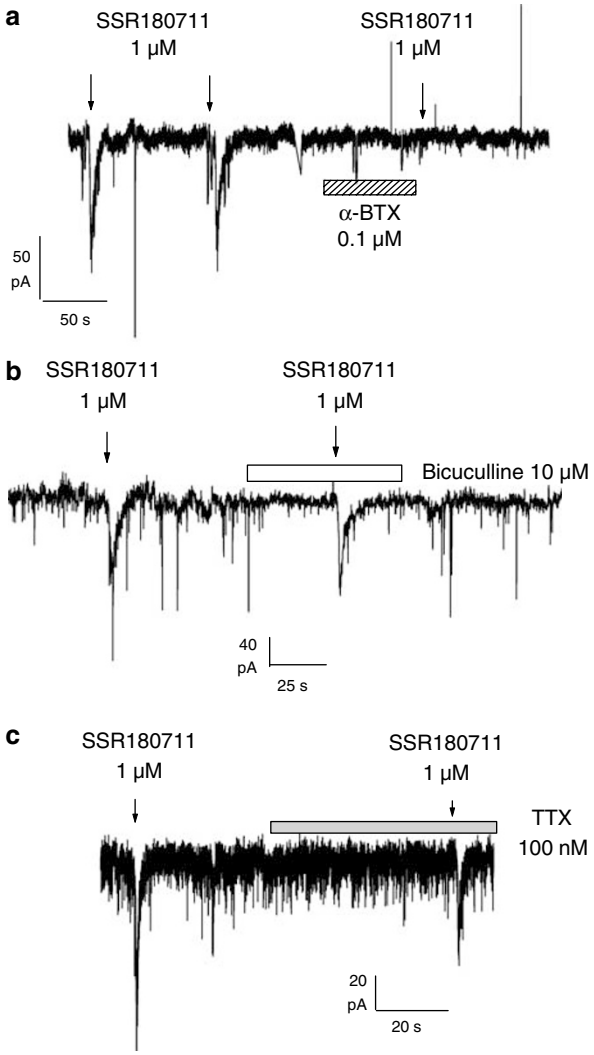

Figure 5 Effect of SSR180711 at rat native somato-dendritic α7 n-AChRs expressed in cultured hippocampal neurons. (a) Variation of the steady-state current as a function of time at a holding potential of −60 mV. SSR180711 at 1 μM induced fast activating inward currents of small amplitudes, completely blocked by α-BTX. In contrast to currents shown in Figure 5, these currents were almost insensitive to TTX (b) and bicuculline (c).

tion of somato-dendritic α7 n-AChRs. Hence, this set of experiments suggests that SSR180711 is effective at native rat hippocampal α7 n-AChRs located at both presynaptic and somato-dendritic locations.

Effect at rat and mouse native α7 n-AChRs expressed in hippocampal slices.

Modulation of electrically evoked glutamatergic EPSCs and GABAergic IPSCs in mouse CA1 pyramidal neurons: Applied at cumulative concentrations until a stable effect was achieved, SSR180711 increased the maximal peak amplitude of the first evoked EPSC of paired eEPSCs (EPSC1 and EPSC2) (Figure 6a). A maximal potentiating effect of EPSC1 peak amplitude by SSR180711 was observed in the 0.3–1 μM range (Figure 6b), the effect lasting as long as the compound was applied, that is several minutes (Figure 6a). At 10 μM of SSR180711, EPSC1 peak amplitude decreased toward values close to control conditions, suggesting a desensitization of α7 n-AChRs (Figure 6a and b). As shown in Figure 6c, SSR180711 induced an increase in the ratio of EPSC2 to EPSC1 maximal amplitudes, suggesting a presynaptic mechanism of action. When the same experiments were performed using mice deficient in the α7 n-AChR gene, SSR180711 was found to be inactive, demonstrating that its effects on glutamatergic neurotransmission were primarily due to an interaction with α7 n-AChRs (Figure 6d, e and f).

SSR180711 also induced a concentration-dependent increase in isolated inhibitory GABAergic eIPSC amplitudes, recorded from wild-type mouse hippocampal slices (Figure 7a). SSR180711 maximally potentiated GABAergic eIPSC in the 0.03–0.1 μM concentration range (Figure 7b). However, the PPR ratio did not clearly indicate a presynaptic mechanism of action, probably due to the lesser stability of eIPSCs amplitudes (Figure 7c). Deletion of α7 n-AChR locus totally abolished the SSR180711-induced effect (Figure 7d, e and f).

Modulation of LTP in rat and mouse hippocampal slices. In vehicle-treated rat hippocampal slices, HFS induced a stable LTP, lasting more than 60 min. In the presence of

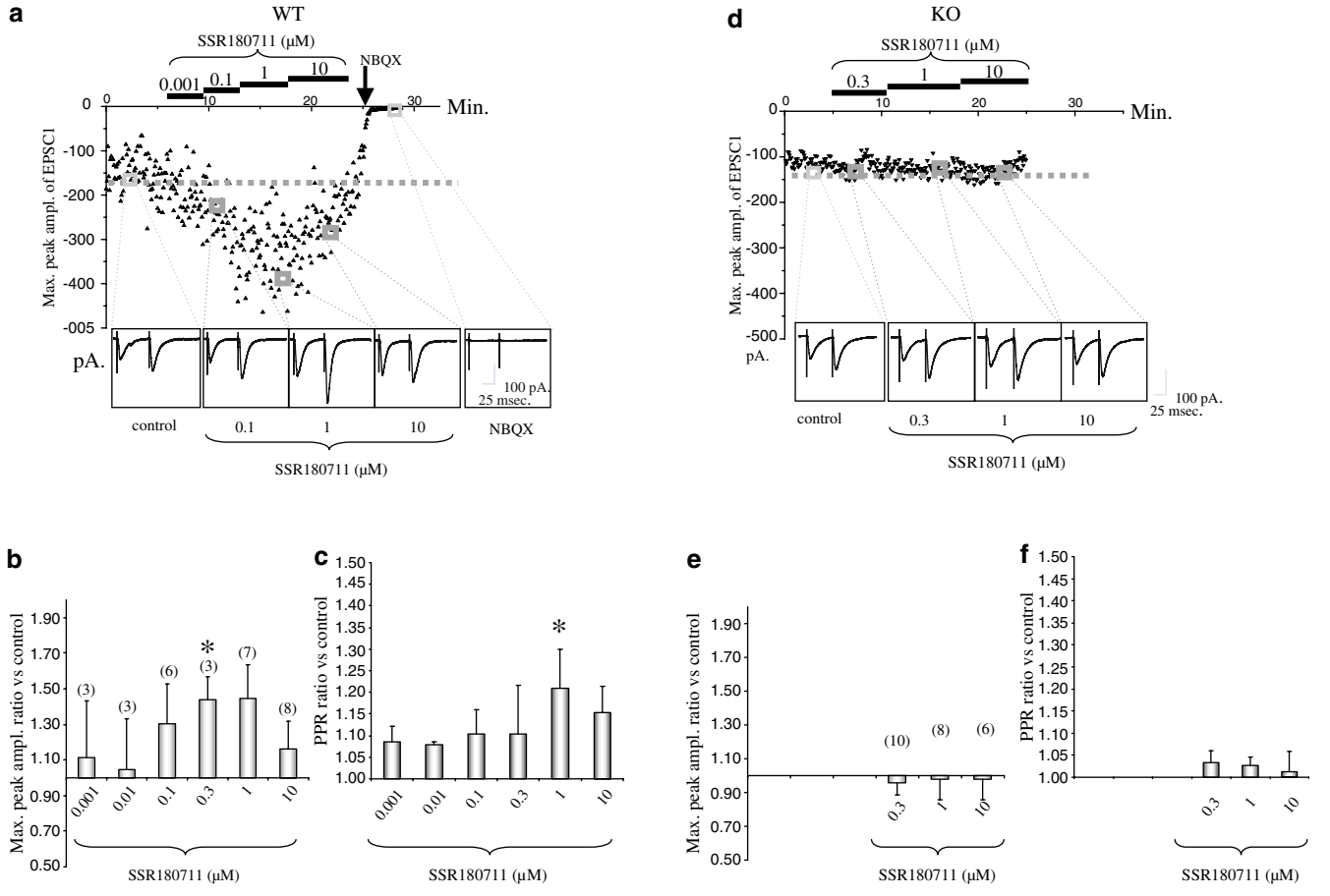

Figure 6 Effect of SSR180711 at glutamatergic EPSCs evoked in mouse hippocampal slices CA1 using paired-pulse protocols. (a) Variation of the maximal amplitude of the first glutamatergic eEPSC (EPSC1, triangles) evoked by a paired pulse protocol (50 ms interval, F = 0.2 Hz) as a function of time and SSR180711 concentrations. Cumulative concentrations of SSR180711 were applied during the time delimited by the black bars. The inserts in the lower part of the figure illustrate original current traces corresponding to the data point shown by the open boxes and dotted lines. NBQX application at the end of the recording demonstrates that eEPSCs are primarily mediated by AMPA and kainate receptors. (b) Summary data, showing the concentration-dependent SSR180711-induced increase in EPSC1 amplitude relative to control (determined during the last minute). (c) Paired Pulse Ratio (PPR) of the second to the first maximal eEPSC amplitude of each pair is plotted as a function of SSR180711 concentration. In conditions similar to those described in (a–c) deletion of α7 n-AChR gene totally abolished SSR180711 effects on eEPSCs (d and e) and on PPR ratio (f). Stars (*) indicate statistically significant difference ($P < 0.05$) using Student paired *t*-test analysis.

300 nM of SSR180711, the mean EPSP amplitude was further increased ($P<0.05$ at 10 and 50 min after HFS). This LTP enhancement was fully antagonized when SSR180711 was superfused in the presence of 100 nM of α-BTX, demonstrating the involvement of α7 n-AChR activation. Superfusion of α-BTX alone had no significant effect *per se*, but surprisingly, a slight increase in LTP was observed during the washout of the toxin, contrasting with the antagonism of SSR180711 effect previously observed (Figure 8).

To further investigate the specificity of SSR180711, similar experiments were performed in wild-type and α7 gene knockout C57bl6/j mice. Invalidation of the gene coding for α7 n-AChR totally abolished the effect of SSR180711 regarding positive modulation of LTP observed in wild-type animals.

Ex Vivo/In Vivo Studies

Ex vivo [^{3}H]α-BTX binding experiments. SSR180711 dose-dependently inhibited the specific [^{3}H]α-BTX binding in the mouse brain when administered orally and i.p. at low doses ($ID_{50}=8.3$ and 7.5 mg/kg, respectively) (Figure 9a). Furthermore, SSR180711 was well absorbed, as shown by the ratio of ID_{50} values obtained after i.p. and oral administrations (ratio = 0.9; Figure 9a). After oral administration SSR180711 (10 mg/kg) induced a rapid inhibition of specific [^{3}H]α-BTX binding that reached, from 15 to 30 min after administration, a floor value of 14% of specific binding. At 4 h after treatment, specific [^{3}H]α-BTX binding returned to basal level indicating that the inhibitory effect of SSR180711 was fully reversible (Figure 9b).

Effects on the firing rate of VP neurons in anesthetized rats. In all, 32 cells were recorded in the VP, whose mean (±SEM) baseline firing rate was 11.57±1.47 (min: 0.41, max: 29.86) spikes/s. As depicted in Figure 10, this firing rate was dose-dependently increased after i.v. administration of SSR180711 (0.1, 0.3, 1 mg/kg). At the dose of 1 mg/kg, this effect was seen from the first 5 min (+196±53% with respect to baseline; $P<0.01$) and reached +339±98% ($P<0.01$) 30 min after administration. It should be noted that in those experiments, all the cells recorded were activated by the doses of 0.3 and 1 mg/kg ($n=5$ and 7, respectively), regardless of their baseline firing rate.

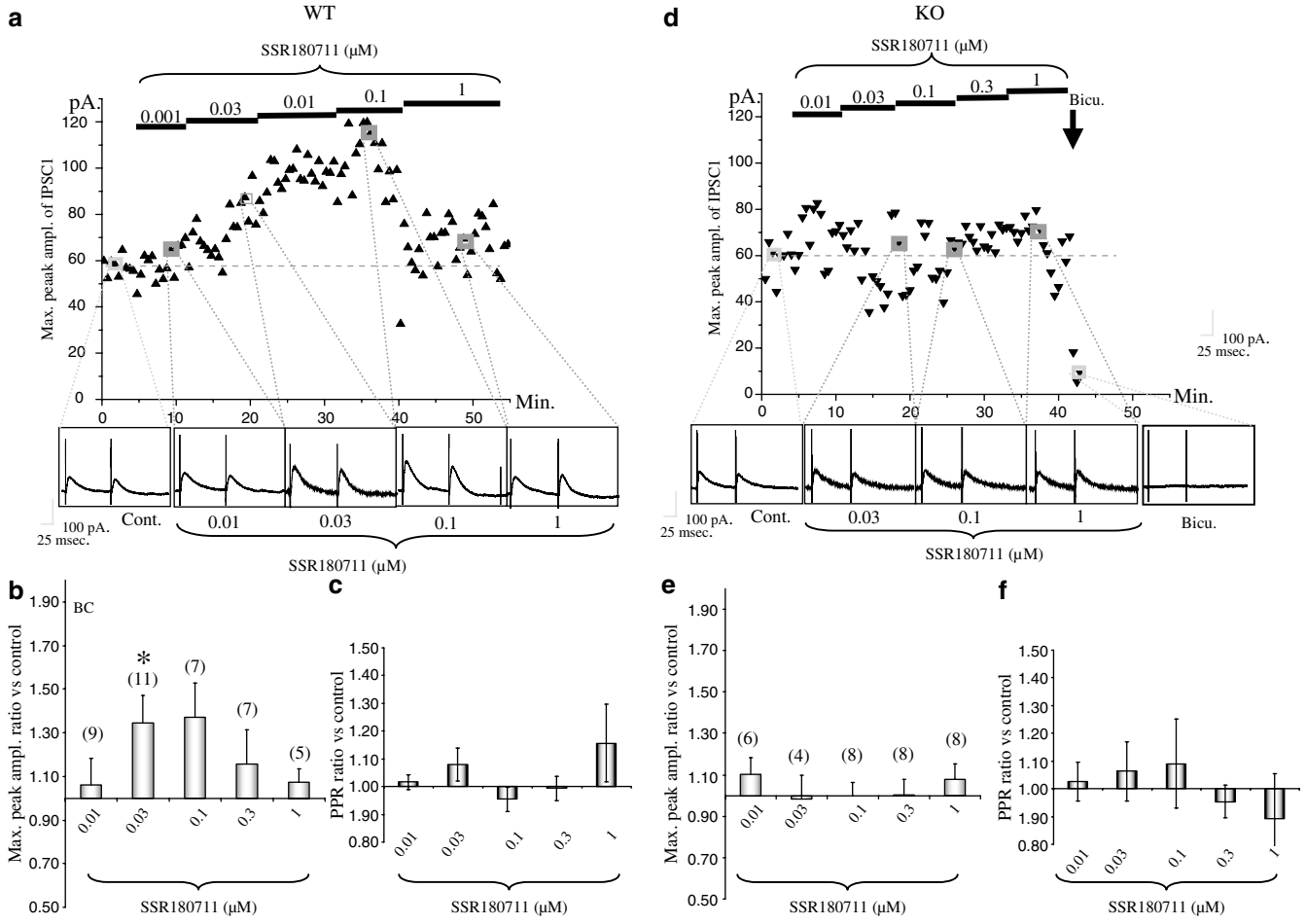

Figure 7 Effect of SSR180711 at GABAergic IPSCs evoked in mouse hippocampal slices CA1 using paired-pulse protocols. (a) Variation of the maximal amplitude of the first GABAergic IPSC (IPSC1, triangles) evoked by a paired pulse protocol (70 ms interval, F = 0.03 Hz) as a function of time and SSR180711 concentrations. Cumulative concentrations of SSR180711 were applied during the time delimited by the black bars. (b) Summary data, showing the concentration-dependent SSR180711-induced increase in IPSC1 amplitude relative to control (determined during the last minute). In wild type (c) and in α7 n-AChR deficient mice (f), SSR180711 did not significantly modify the PPR. (d and e) In conditions similar to those described in (a and b), deletion of α7 n-AChR gene totally abolished SSR180711 effects on eIPSCs. Stars (*) indicate statistically significant difference ($P<0.05$) using Student paired *t*-test analysis.

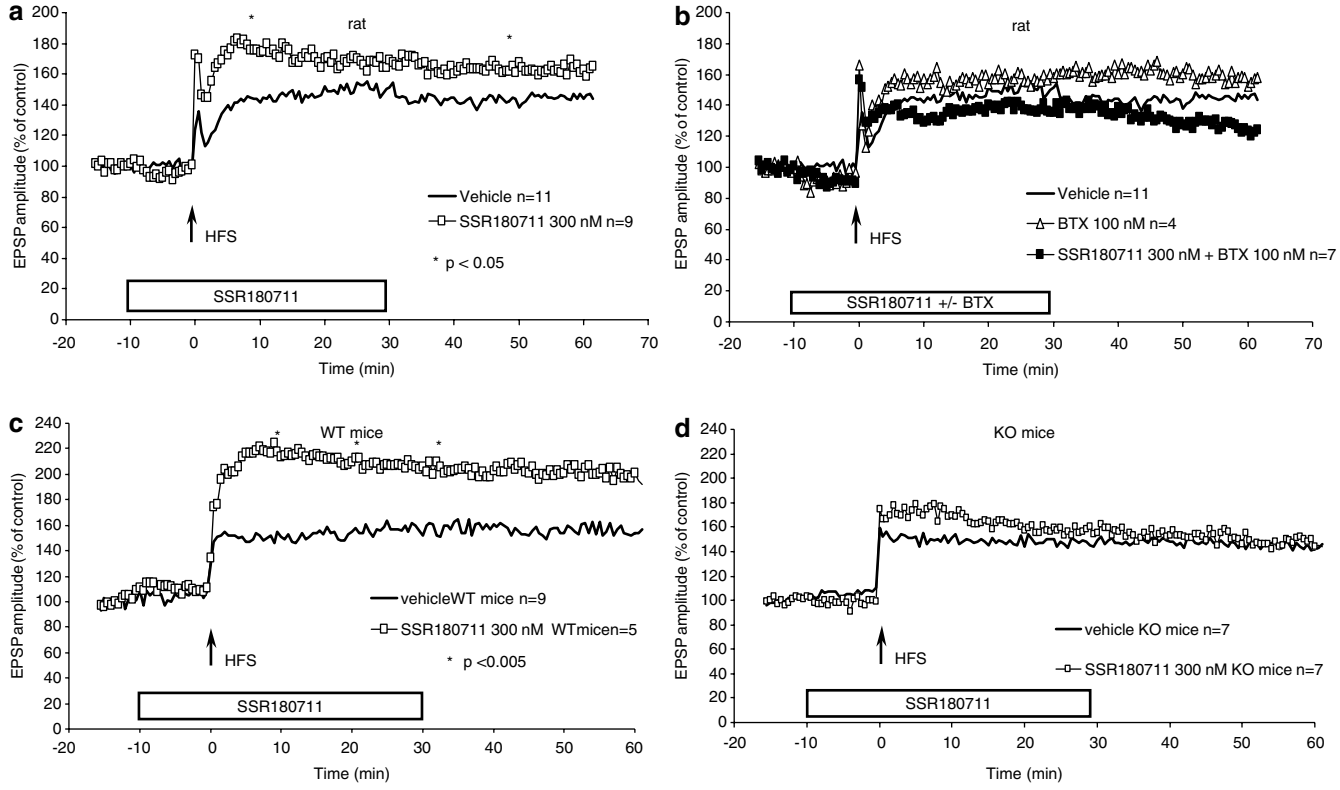

Figure 8 SSR180711 increased HFS-induced LTP in CA1 neurons in slices from rat or wild type mice (WT) hippocampus by selective activation of α7-nicotinic receptors. In rat hippocampal slices (a), SSR180711 at 0.3 μM significantly increased LTP while it remained unchanged in the presence of -α-bungarotoxin (b). In WT mouse hippocampal slices (c), SSR180711 at 0.3 μM also significantly increased LTP while no effect was observed in α7 n-AChR deficient mice (d). Compounds were superfused at the indicated concentrations during the time shown by the open boxes that is; 10 min before and 30 min after LTP induction. Stars (*) indicate statistically significant difference ($P<0.05$) compared to control. Abbreviations: HFS: high-frequency stimulation; BTX: α-bungarotoxin. Standard deviation bars were omitted for clarity.

MLA (0.3 mg/kg i.v.) was administered either alone or 30 min after SSR180711 (1 mg/kg i.v.). The spontaneous firing rate of VP cells was unaffected by MLA alone (Figure 10), but this drug completely blocked the enhancing effects of SSR180711 (1 mg/kg i.v.), with a maximum fall of $92.5\pm3.0\%$ (15 min; with respect to pre-MLA level, $P<0.01$).

As also illustrated in Figure 10, the spontaneous firing rate of VP cells was unaffected by the administration of a low dose of MK-801 alone (0.03 mg/kg i.v.). However, this drug fully reversed the increase in firing rate induced by prior application (15 min) of SSR180711 (1 mg/kg i.v.), with a maximum $88.8\pm3.2\%$ ($P<0.01$) drop 10 min after MK-801 administration.

Effects on extracellular levels of ACh in the hippocampus and prefrontal cortex of freely moving rats. The average basal extracellular ACh levels in the hippocampus and prefrontal cortex were estimated to be 0.76 ± 0.10 pmol ($n=19$) and 0.67 ± 0.07 pmol ($n=17$), respectively. SSR180711 (i.p. route) produced significant ($F(7,105)=3.27$, $P<0.05$ and $F(7,95)=4.04$, $P<0.01$, for the hippocampus and prefrontal cortex, respectively) and dose-dependent increases in ACh release (Figure 11a and b). Maximal increases were $190\pm30\%$ at 40 min for the dose of 10 mg/kg, i.p. in the hippocampus and $176\pm23\%$ of basal value at 60 min for the dose of 3 mg/kg, i.p. in the prefrontal cortex). SSR180711 (p.o. route) also produced significant ($F(6, 108)=15.57$, $P<0.01$) and dose-dependent increases in cortical ACh release with a maximal effect of $212\pm39\%$ of basal value at 40 min for the dose of 30 mg/kg, p.o. (Figure 11c).

DISCUSSION

The present study investigated the pharmacological properties of the novel selective α7 n-AChR partial agonist, SSR180711. The drug displays high affinity for the rat and human α7 n-AChR subtype ($IC_{50}=30$ and 18 nM, respectively), whereas it shows much weaker affinity for other n-AChR subtypes as demonstrated by binding and patch-clamp experiments (selectivity ratio >250-fold when compared to IC_{50} values obtained for hα4β2, hα3β2, hα3β4, or α1β1γδ n-AChRs). Furthermore, SSR180711 was studied at 10 μM in a 100-standard receptor binding profile (CEREP), where no detectable activity for various ion channels, neurotransmitter or peptide receptors was found (data not shown).

Recent data have demonstrated that heteromeric assembly of recombinant α7 and β2 subunits could form functional receptors, displaying some pharmacological differences with homomeric ones (Azam *et al*, 2003; Khiroug *et al*, 2002). Given the high expression level of α7 and β2 subunits in the hippocampus, it was therefore of interest to

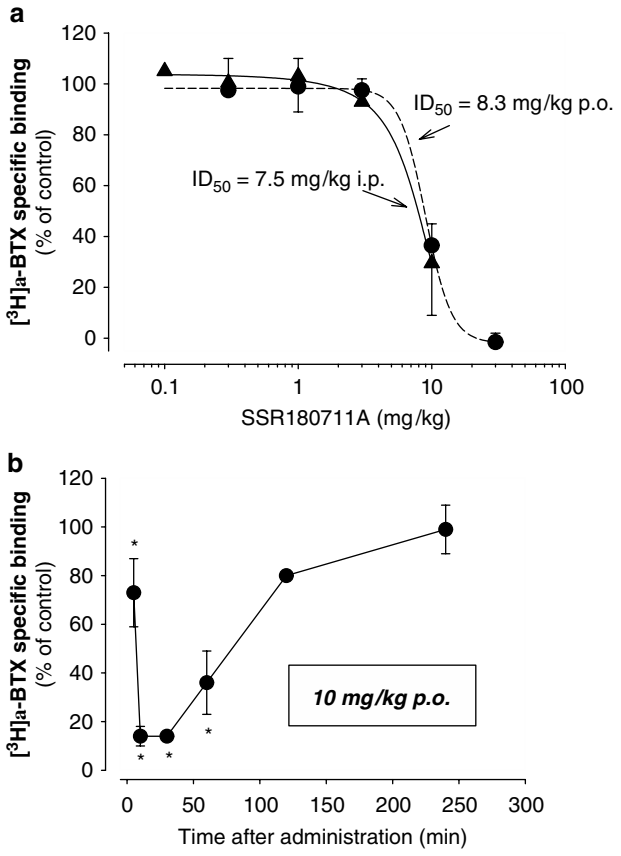

Figure 9 *Ex vivo* characterization of SSR180711 interaction with mouse α7 n-AChRs. (a) Comparative effects of i.p. and oral treatment by SSR180711 on *ex vivo* [3H]α-BTX binding in the mouse cortex. Data values are obtained from two determinations for each treatment. (b) Kinetic study of the effect of an oral administration of SSR180711 (10 mg/kg) on *in vivo* [^{3}H]α-BTX binding in the mouse cortex ($n = 3$ animals per experimental group). *$P < 0.05$, Kruskal–Wallis *post hoc* test *vs* time treatment of control group.

test the activity and efficacy of SSR180711 at native α7 n-AChRs in cultured hippocampal neurons, possibly formed of a mixture of homomeric and heteromeric receptors (Azam *et al*, 2003). In rat cultured hippocampal neurons, whole-cell recordings have shown that SSR180711 could induce two types of responses, depending on their sensitivity to TTX and bicuculline. These differences were attributed to an agonist effect of SSR180711 at two types of α7 n-AChRs, identified as presynaptic or somato-dendritic, since both types of response were blocked by α-BTX. This finding also indicates that homomeric and heteromeric receptors either display similar sensitivity to this compound or do not discriminate between a presynaptic or a somato-dendritic localization. The fact that very similar IC_{50} values were found in ^{3}[H]α-BTX binding experiments at recombinant human and rat native α7 n-AChRs (the former being homomeric and the latter being possibly heteromeric) reinforces the hypothesis that SSR180711 does not discriminate between the two forms of receptors, if they do exist in native tissues. Indeed, data obtained in binding experiments performed with rat or mouse brain membranes was better approximated by a one-site model. This should not be the case if different subtypes of α7 n-AChRs were present (Cuevas *et al*, 2000), although this may be related to the experimental conditions employed in the binding assay.

When functionally studied at human α7 n-AChRs transiently expressed either in *Xenopus* oocytes or in GH4C1 cells, SSR180711 was found to behave as a partial agonist with an intrinsic activity of 51 and 36%, respectively, and EC_{50} values of 4.4 and 0.9 μM, respectively. These slight differences are probably linked to the different cell models used in these experiments. Indeed, it is a common finding that the oocyte expression system is one order of magnitude less sensitive than recombinant mammalian systems. The fact that in these electrophysiological experiments, SSR180711 induced currents independently of any exogenously added agonist suggests that the compound recognizes the orthosteric site of the receptor, although an additional effect through an allosteric site cannot be ruled out at the present time.

Another important feature of the agonist profile of SSR180711 is its short-lasting desensitizing properties, as demonstrated by the rapid recovery of ACh-induced currents following SSR180711 application observed in both models. Desensitization of α7 n-AChRs is likely to be a crucial parameter when considering experimental conditions in which α7 n-AChRs are acted upon by an agonist for a long period of time, as it is the case during chronic treatment. In this respect, additional experiments aimed at describing the effect of continuous superfusion of SSR180711 with transient application of ACh or choline at α7 n-AChR would be necessary to better assess the desensitizing properties of the compound. However, exogenous agonists such as SSR180711 may also act as extrasynaptic α7 n-AChRs, shown to be predominant in some neural structures, suggesting that an exogenous agonist could be active without competing against synaptically released ACh (Jones and Wonnacott, 2004; Coggan *et al*, 2005). At a more integrated levels and as mentioned in the Introduction section, it is still unclear whether the excitatory effects of α7 n-AChR agonists described in the hippocampus do involve an activation of glutamate release (via activation of α7 n-AChRs) or a decrease of GABA release (by desensitization of α7 n-AChRs) (Fujii *et al*, 2000; Gray *et al*, 1996; Hunter *et al*, 1994). Indeed, the electrophysiological experiments conducted in hippocampal slices show that SSR180711 superfused for several minutes in a cumulative concentration procedure, induced a concentration-dependent increase of eEPSCs, with a maximal effect observed for concentrations between 0.3 and 1 μM, the effect being of lower amplitude at 10 μM. As in these experiments, GABA(A) receptor-mediated transmission was blocked by bicuculline, it is very likely that the observed effects were due to an increase in glutamate release via the activation of α7 n-AChRs. The results of LTP experiments in hippocampal slices also strongly support the hypothesis that SSR180711-induced enhancement of glutamatergic neurotransmission is mediated by the stimulation of α7 n-AChRs and not by their desensitization. Indeed, SSR180711-induced stimulating effects were completely prevented by superfusion of the α7 n-AChR antagonist, α-BTX. Blockade of α7 n-AChRs—functionally similar to a full desensitization—had no stimulating effect *per se* at glutamatergic neurotransmission since α-BTX superfusion did not induce

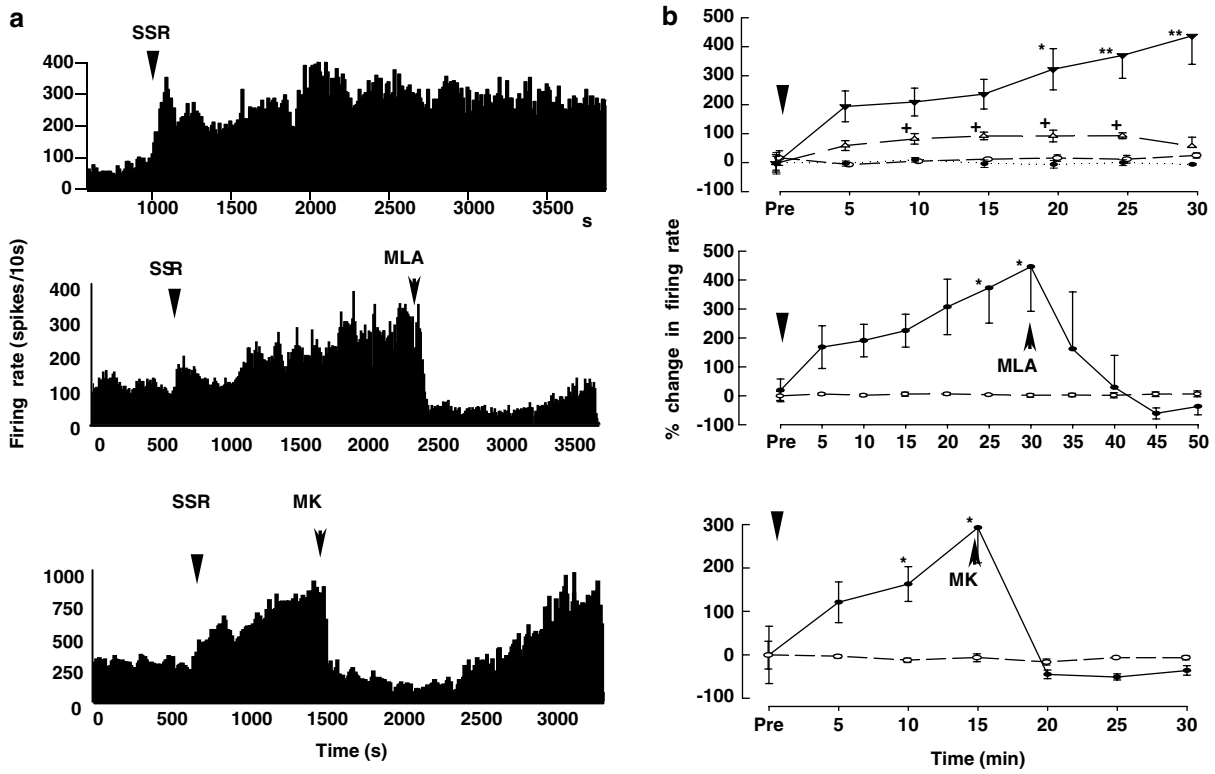

Figure 10 SSR180711 increased the firing rate of VP cells in anesthetized rats in a MLA- and MK-801-sensitive manner. (a) Typical samples of firing rate histograms showing (from top to bottom) the enhancing effect of SSR180711 (SSR; 1 mg/kg i.v.) and its reversal by MLA (0.3 mg/kg i.v.) and MK-801 (MK; 0.03 mg/kg i.v.), respectively. (b) Top: dose–response effects of SSR180711 at 0.1 (open circles; $n=4$), 0.3 (open triangles; $n=5$) and 1 mg/kg i.v. (filled triangles; $n=7$) on the firing rate of VP cells. No change was noted with vehicle alone (filled circles; $n=4$). Middle: reversal by MLA (0.3 mg/kg i.v.) of SSR180711 (1 mg/kg i.v.)-induced increase of firing rate (filled circles; $n=4$). MLA by itself was ineffective (open circles; $n=4$). Bottom: reversal by MK-801 (0.03 mg/kg i.v.) of SSR180711 (1 mg/kg i.v.)-induced increase of firing rate (filled circles; $n=4$). MK-801 had no effect at this dose (open circles; $n=4$). All curves express the mean (±SEM) % changes (ordinates) with respect to baseline (Pre; 0%) firing values, as a function of time (abscissae); n = number of cells recorded (a single cell per rat). Arrows indicate i.v. administrations. $^{*,+}P<0.05$; $^{**}P<0.01$ (with respect to predrug values; paired ANOVA followed by Duncan's multiple comparison test applied to raw firing rate values).

a significant modification of LTP or basal synaptic transmission, despite a slight but nonsignificant increase in LTP during α-BTX washout. It has been suggested that both desensitization of α7 n-AChRs and activation of non α7 n-AChRs could contribute to the LTP induced in the CA1 region of the hippocampus (Fujii *et al*, 2000). In these experiments, the authors used nicotine as a reference agonist and it was found that MLA (an antagonist of α7 n-AChRs) could facilitate LTP induction, while dihydro-β-erythroidin (an antagonist of α4β2 n-AChRs) preapplication completely prevented it. These discrepancies between our results and those of Fujii *et al*, may be explained by the use of different α7 n-AChR agonists and antagonists. Indeed, nicotine is a large spectrum agonist at n-AChRs, activating nondiscriminatively α4β2, α7, α3β2, α2β4, α3β4 n-AChRs while SSR180711 is a selective agonist of α7 n-AChRs. In addition, experiments conducted in α7-KO mice demonstrate that SSR180711 directly increases glutamate release and LTP via a specific effect at α7 n-AChRs. Finally, the observation of a similar level of LTP in wild-type and α7-KO mice rules out the hypothesis of a tonic inhibitory input mediated by α7 n-AChRs. Together, these data strongly support the hypothesis that SSR180711 directly increases glutamate release and LTP via the activation of α7 n-AChRs.

In the hippocampus, an increase in GABAergic transmission has also frequently been reported after stimulation of nicotinic receptors, in accordance with the well-documented expression of α7 n-AChRs on GABAergic interneurons (Alkondon *et al*, 1999; Buhler and Dunwiddie, 2002). In good agreement with these findings, SSR180711 was found to induce a strong activation of spontaneous GABA-induced currents in cultured hippocampal neurons and a concentration-dependent increase in the amplitude of eIPSCs recorded in the CA1 field of mouse hippocampal slices, with a maximal effect in the 0.03–0.1 μM range. No modification of eIPSCs was observed when SSR180711 was studied in slices prepared from α7-KO mice, further demonstrating the involvement of α7 n-AChRs.

Discrepancies between SSR180711 concentrations achieving maximal potentiation of eIPSCs and eEPSCs could be explained by the presence of bicuculline in the external medium for eEPSC experiments. Indeed, bicuculline has been described as a weak α7 n-AChRs antagonist, thus possibly leading to an underestimation of the potentiating effect of SSR180711 in eEPSCs studies (Demuro *et al*, 2001). Moreover, the frequency of stimulation was much higher in eEPSC than in eIPSC protocols, which could increase spontaneous ACh release, leading to a decrease in the sensitivity of the preparation to SSR180711.

In addition, *in vivo* experiments in anesthetized rats have shown that SSR180711 increases the firing rate of VP neurons, this effect being blocked by the selective α7

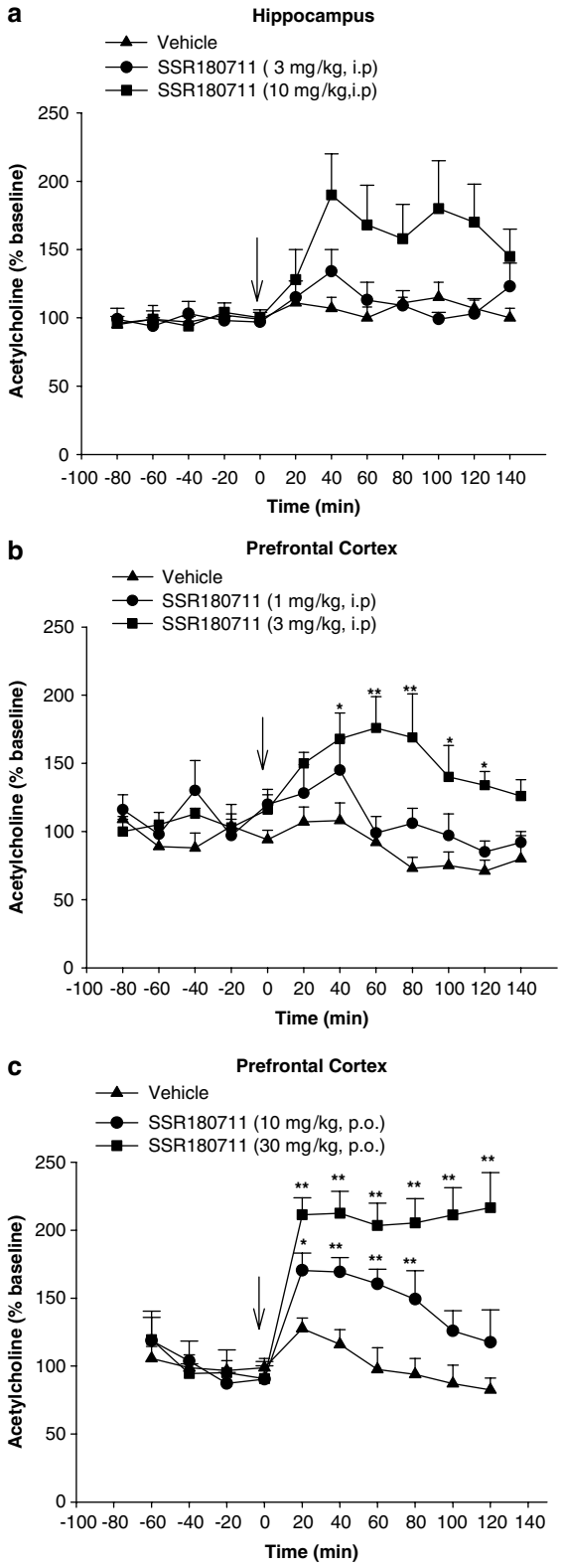

Figure 11 Effect of SSR180711 of extracellular ACh levels in the hippocampus and prefrontal cortex of freely moving rats. Changes in extracellular levels of ACh are expressed as a percentage of the mean value of the four basal samples before administration of SSR180711 or vehicle (indicated by a vertical arrow). Each symbol represents the mean + SEM. $^{*}P<0.05$, $^{**}P<0.01$ *vs* the vehicle value at the corresponding time of sampling, Dunnetts' *post hoc* tests following a two-way ANOVA. $N=5$–9 rats per group.

n-AChR antagonist MLA and by the selective NMDA receptor antagonist, MK-801. This observation strongly suggests that, in the involved circuitry, an increase in glutamate release via α7 n-AChRs mediates the activation of VP neurons. The VP belongs to the basal forebrain (BF), a complex of areas which, through reciprocal connections with prefrontal and limbic cortices, is involved in higher cognitive and memory functions. Although the nature of the VP cells recorded in the present study was not determined, their firing frequencies were similar to those described for identified cholinergic and GABAergic neurons recorded in the VP and other BF nuclei in previous studies (Golmayo *et al*, 2003). Those cholinergic and GABAergic neurons have been shown to project to cortical pyramidal cells and GABAergic interneurons, respectively (Furuta *et al*, 2004; Golmayo *et al*, 2003; Gritti *et al*, 1997). SSR180711-induced activation of VP cells is thus likely to result in global facilitating processes at the cortical level, through both excitatory and disinhibitory drives. This is supported (see companion paper) by the activating effects of SSR180711 on neurons of the retrosplenial cortex, a limbic cortical region involved in spatial memory (Harker and Whishaw, 2002). When GABAergic eIPSCs were studied in mouse hippocampal slices, the glutamatergic neurotransmission was blocked, using high concentrations of 2-APV and NBQX (see Materials and methods section). These *in vivo* and *in vitro* results therefore suggest that SSR180711-induced modulation of GABAergic neurotransmission may involve both direct activation of α7 n-AChRs and an indirect effect via the activation of NMDA receptors.

Brain penetration and gastro-intestinal absorption are crucial issues for any drug intended to treat CNS diseases. *Ex vivo* [^{3}H]α-BTX binding experiments in mice demonstrated that SSR180711 effectively penetrates the brain with a ratio i.p./p.o. of 0.9, suggesting that this compound is orally biovailable in the rat. Indeed, SSR180711 increased extracellular ACh levels in rat hippocampus and prefrontal cortex *in vivo* and in the latter region the dose of 10 mg/kg, p.o. was as efficacious as the dose of 3 mg/kg, i.p. The mechanism whereby SSR180711 induces this effect on extracellular ACh levels (ie direct or indirect effect at cholinergic neurons) deserves further studies.

In conclusion, this study shows that SSR180711 is a selective and potent partial agonist at recombinant and native α7 n-AChRs, enhancing glutamatergic EPSCs and LTP in the hippocampus. Moreover, *in vivo* electrophysiological studies in the VP suggest that SSR180711 could induce a facilitation of systems involved in higher brain functions. Finally when administered orally, SSR180711 increased ACh release in hippocampus and prefrontal cortex. Taken together, these results suggest that SSR180711 represents a promising candidate for the treatment of disorders associated with cognitive/attention deficits.

ACKNOWLEDGEMENTS

We thank Thibault De Gallier, Catherine Marc and Nicole Brunel for their excellent technical assistance, Jean-Michel Lefevre for having provided transgenic mice, Véronique Onado and Mathieu Rose for their helpful contribution to data analysis.

REFERENCES

Alkondon M, Braga MF, Pereira EF, Maelicke A, Albuquerque EX (2000). alpha7 nicotinic acetylcholine receptors and modulation of gabaergic synaptic transmission in the hippocampus. *Eur J Pharmacol* **393**: 59–67.

Alkondon M, Pereira EF, Eisenberg HM, Albuquerque EX (1999). Choline and selective antagonists identify two subtypes of nicotinic acetylcholine receptors that modulate GABA release from CA1 interneurons in rat hippocampal slices. *J Neurosci* **19**: 2693–2705.

Azam L, Winzer-Serhan U, Leslie FM (2003). Co-expression of alpha7 and beta2 nicotinic acetylcholine receptor subunit mRNAs within rat brain cholinergic neurons. *Neuroscience* **119**: 965–977.

Buhler AV, Dunwiddie TV (2002). alpha7 nicotinic acetylcholine receptors on GABAergic interneurons evoke dendritic and somatic inhibition of hippocampal neurons. *J Neurophysiol* **87**: 548–557.

Canton T, Bohme GA, Boireau A, Bordier F, Mignani S, Jimonet P *et al* (2001). RPR 119990, a novel alpha-amino-3-hydroxy-5-methyl-4-isoxazolepropionic acid antagonist: synthesis, pharmacological properties, and activity in an animal model of amyotrophic lateral sclerosis. *J Pharmacol Exp Ther* **299**: 314–322.

Cheng Y, Prusoff WH (1973). Relationship between the inhibition constant (K1) and the concentration of inhibitor which causes 50 per cent inhibition (I50) of an enzymatic reaction. *Biochem Pharmacol* **22**: 3099–3108.

Coggan JS, Bartol TM, Esquenazi E, Stiles JR, Lamont S, Martone ME *et al* (2005). Evidence for ectopic neurotransmission at a neuronal synapse. *Science* **309**: 446–451.

Court J, Spurden D, Lloyd S, McKeith I, Ballard C, Cairns N *et al* (1999). Neuronal nicotinic receptors in dementia with Lewy bodies and schizophrenia: alpha-bungarotoxin and nicotine binding in the thalamus. *J Neurochem* **73**: 1590–1597.

Court JA, Ballard CG, Piggott MA, Johnson M, O'Brien JT, Holmes C *et al* (2001). Visual hallucinations are associated with lower alpha bungarotoxin binding in dementia with Lewy bodies. *Pharmacol Biochem Behav* **70**: 571–579.

Cuevas J, Roth AL, Berg DK (2000). Two distinct classes of functional 7-containing nicotinic receptor on rat superior cervical ganglion neurons. *J Physiol* **525**(Part 3): 735–746.

De Luca V, Wang H, Squassina A, Wong GW, Yeomans J, Kennedy JL (2004a). Linkage of M5 muscarinic and alpha7-nicotinic receptor genes on 15q13 to schizophrenia. *Neuropsychobiology* **50**: 124–127.

De Luca V, Wong AH, Muller DJ, Wong GW, Tyndale RF, Kennedy JL (2004b). Evidence of association between smoking and alpha7 nicotinic receptor subunit gene in schizophrenia patients. *Neuropsychopharmacology* **29**: 1522–1526.

Demuro A, Palma E, Eusebi F, Miledi R (2001). Inhibition of nicotinic acetylcholine receptors by bicuculline. *Neuropharmacology* **41**: 854–861.

Dineley KT, Bell KA, Bui D, Sweatt JD (2002). Beta-Amyloid peptide activates alpha 7 nicotinic acetylcholine receptors expressed in *Xenopus* oocytes. *J Biol Chem* **277**: 25056–25061.

Dougherty JJ, Wu J, Nichols RA (2003). Beta-amyloid regulation of presynaptic nicotinic receptors in rat hippocampus and neocortex. *J Neurosci* **23**: 6740–6747.

Fabian-Fine R, Skehel P, Errington ML, Davies HA, Sher E, Stewart MG *et al* (2001). Ultrastructural distribution of the alpha7 nicotinic acetylcholine receptor subunit in rat hippocampus. *J Neurosci* **21**: 7993–8003.

Flesher JE, Scheffel U, London ED, Frost JJ (1994). *In vivo* labeling of nicotinic cholinergic receptors in brain with [3H]cytisine. *Life Sci* **54**: 1883–1890.

Frazier CJ, Buhler AV, Weiner JL, Dunwiddie TV (1998). Synaptic potentials mediated via alpha-bungarotoxin-sensitive nicotinic acetylcholine receptors in rat hippocampal interneurons. *J Neurosci* **18**: 8228–8235.

Freedman R, Adams CE, Leonard S (2000). The alpha7-nicotinic acetylcholine receptor and the pathology of hippocampal interneurons in schizophrenia. *J Chem Neuroanat* **20**: 299–306.

Freedman R, Leonard S, Gault JM, Hopkins J, Cloninger CR, Kaufmann CA *et al* (2001). Linkage disequilibrium for schizophrenia at the chromosome 15q13-14 locus of the alpha7-nicotinic acetylcholine receptor subunit gene (CHRNA7). *Am J Med Genet* **105**: 20–22.

Fujii S, Ji Z, Sumikawa K (2000). Inactivation of alpha7 ACh receptors and activation of non-alpha7 ACh receptors both contribute to long term potentiation induction in the hippocampal CA1 region. *Neurosci Lett* **286**: 134–138.

Furuta T, Koyano K, Tomioka R, Yanagawa Y, Kaneko T (2004). GABAergic basal forebrain neurons that express receptor for neurokinin B and send axons to the cerebral cortex. *J Comp Neurol* **473**: 43–58.

Golmayo L, Nunez A, Zaborszky L (2003). Electrophysiological evidence for the existence of a posterior cortical-prefrontal-basal forebrain circuitry in modulating sensory responses in visual and somatosensory rat cortical areas. *Neuroscience* **119**: 597–609.

Gopalakrishnan M, Monteggia LM, Anderson DJ, Molinari EJ, Piattoni-Kaplan M, Donnelly-Roberts D *et al* (1996). Stable expression, pharmacologic properties and regulation of the human neuronal nicotinic acetylcholine alpha 4 beta 2 receptor. *J Pharmacol Exp Ther* **276**: 289–297.

Grassi F, Palma E, Tonini R, Amici M, Ballivet M, Eusebi F (2003). Amyloid beta(1-42) peptide alters the gating of human and mouse alpha-bungarotoxin-sensitive nicotinic receptors. *J Physiol* **547**: 147–157.

Gray R, Rajan AS, Radcliffe KA, Yakehiro M, Dani JA (1996). Hippocampal synaptic transmission enhanced by low concentrations of nicotine. *Nature* **383**: 713–716.

Gritti I, Mainville L, Mancia M, Jones BE (1997). GABAergic and other noncholinergic basal forebrain neurons, together with cholinergic neurons, project to the mesocortex and isocortex in the rat. *J Comp Neurol* **383**: 163–177.

Harker KT, Whishaw IQ (2002). Impaired spatial performance in rats with retrosplenial lesions: importance of the spatial problem and the rat strain in identifying lesion effects in a swimming pool. *J Neurosci* **22**: 1155–1164.

Hunter BE, de Fiebre CM, Papke RL, Kem WR, Meyer EM (1994). A novel nicotinic agonist facilitates induction of long-term potentiation in the rat hippocampus. *Neurosci Lett* **168**: 130–134.

Jones IW, Wonnacott S (2004). Precise localization of alpha7 nicotinic acetylcholine receptors on glutamatergic axon terminals in the rat ventral tegmental area. *J Neurosci* **24**: 11244–11252.

Khiroug SS, Harkness PC, Lamb PW, Sudweeks SN, Khiroug L, Millar NS *et al* (2002). Rat nicotinic ACh receptor alpha7 and beta2 subunits co-assemble to form functional heteromeric nicotinic receptor channels. *J Physiol* **540**: 425–434.

Kihara T, Sawada H, Nakamizo T, Kanki R, Yamashita H, Maelicke A *et al* (2004). Galantamine modulates nicotinic receptor and blocks Abeta-enhanced glutamate toxicity. *Biochem Biophys Res Commun* **325**: 976–982.

Lanneau C, Harries MH, Ray AM, Cobb SR, Randall A, Davies CH (2002). Complex interactions between mGluR1 and mGluR5 shape neuronal network activity in the rat hippocampus. *Neuropharmacology* **43**: 131–140.

Lowry OH, Rosebrough NJ, Farr AL, Randall RJ (1951). Protein measurement with the Folin phenol reagent. *J Biol Chem* **193**: 265–275.

Lukas RJ (1986). Characterization of curaremimetic neurotoxin binding sites on membrane fractions derived from the human medulloblastoma clonal line, TE671. *J Neurochem* **46**: 1936–1941.

Lukas RJ (1993). Expression of ganglia-type nicotinic acetylcholine receptors and nicotinic ligand binding sites by cells of the IMR-32 human neuroblastoma clonal line. *J Pharmacol Exp Ther* **265**: 294–302.

Lukas RJ, Morimoto H, Bennett EL (1979). Effects of thio-group modification and Ca2+ on agonist-specific state transitions of a central nicotinic acetylcholine receptor. *Biochemistry* **18**: 2384–2395.

Marchi M, Risso F, Viola C, Cavazzani P, Raiteri M (2002). Direct evidence that release-stimulating alpha7 nicotinic cholinergic receptors are localized on human and rat brain glutamatergic axon terminals. *J Neurochem* **80**: 1071–1078.

Marks MJ, Stitzel JA, Romm E, Wehner JM, Collins AC (1986). Nicotinic binding sites in rat and mouse brain: comparison of acetylcholine, nicotine, and alpha-bungarotoxin. *Mol Pharmacol* **30**: 427–436.

Nelson ME, Wang F, Kuryatov A, Choi CH, Gerzanich V, Lindstrom J (2001). Functional properties of human nicotinic AChRs expressed by IMR-32 neuroblastoma cells resemble those of alpha3beta4 AChRs expressed in permanently transfected HEK cells. *J Gen Physiol* **118**: 563–582.

Nishizaki T, Matsuoka T, Nomura T, Kondoh T, Watabe S, Shiotani T *et al* (2000). Presynaptic nicotinic acetylcholine receptors as a functional target of nefiracetam in inducing a long-lasting facilitation of hippocampal neurotransmission. *Alzheimer Dis Assoc Disord* **14**(Suppl 1): S82–S94.

Nordberg A (2001). Nicotinic receptor abnormalities of Alzheimer's disease: therapeutic implications. *Biol Psychiatry* **49**: 200–210.

Orr-Urtreger A, Goldner FM, Saeki M, Lorenzo I, Goldberg L, De Biasi M *et al* (1997). Mice deficient in the alpha7 neuronal nicotinic acetylcholine receptor lack alpha-bungarotoxin binding sites and hippocampal fast nicotinic currents. *J Neurosci* **17**: 9165–9171.

Pabreza LA, Dhawan S, Kellar KJ (1991). 3H]cytisine binding to nicotinic cholinergic receptors in brain. *Mol Pharmacol* **39**: 9–12.

Parker MJ, Beck A, Luetje CW (1998). Neuronal nicotinic receptor beta2 and beta4 subunits confer large differences in agonist binding affinity. *Mol Pharmacol* **54**: 1132–1139.

Paxinos G, Watson C (1998). *The Rat Brain in Stereotaxic Coordinates*, 4th edn. Academic Press: New York.

Perry EK, Martin-Ruiz CM, Court JA (2001). Nicotinic receptor subtypes in human brain related to aging and dementia. *Alcohol* **24**: 63–68.

Pichat P, Bergis OE, Terranova JP, Duarte C, Santucci V, Gueudet C *et al* (2006). SSR180711A, a novel selective 7 nicotinic receptor partial agonist: II) Efficacy in experimental models predictive of activity against cognitive symptoms of schizophrenia. *Neuropsychopharmacology*, advance online publication, August 23, 2006; doi:10.1038/sj.npp.1301188.

Quik M, Choremis J, Komourian J, Lukas RJ, Puchacz E (1996). Similarity between rat brain nicotinic alpha-bungarotoxin receptors and stably expressed alpha-bungarotoxin binding sites. *J Neurochem* **67**: 145–154.

Radcliffe KA, Fisher JL, Gray R, Dani JA (1999). Nicotinic modulation of glutamate and GABA synaptic transmission of hippocampal neurons. *Ann NY Acad Sci* **868**: 591–610.

Reno LA, Zago W, Markus RP (2004). Release of [(3)H]-L-glutamate by stimulation of nicotinic acetylcholine receptors in rat cerebellar slices. *Neuroscience* **124**: 647–653.

Rezvani AH, Levin ED (2001). Cognitive effects of nicotine. *Biol Psychiatry* **49**: 258–267.

Sawada S, Ohno-Shosaku T, Yamamoto C (1994). Augmenting action of nicotine on population spikes in the dentate gyrus of the guinea pig. *Neurosci Res* **20**: 317–322.

Schoepfer R, Luther M, Lindstrom J (1988). The human medulloblastoma cell line TE671 expresses a muscle-like acetylcholine receptor. Cloning of the alpha-subunit cDNA. *FEBS Lett* **226**: 235–240.

Severance EG, Cuevas J (2004). Distribution and synaptic localization of nicotinic acetylcholine receptors containing a novel alpha7 subunit isoform in embryonic rat cortical neurons. *Neurosci Lett* **372**: 104–109.

Steinberg R, Rodier D, Souiclhac J, Bougault I, Emonds-Alt X, Soubrie P *et al* (1995). Pharmacological characterization of tachykinin receptors controlling acetylcholine release from rat striatum: an *in vivo* microdialysis study. *J Neurochem* **65**: 2543–2548.

Stip E, Chouinard S, Boulay LJ (2005). On the trail of a cognitive enhancer for the treatment of schizophrenia. *Prog Neuropsychopharmacol Biol Psychiatry* **29**: 219–232.

Strong R, Reddy V, Morley JE (2003). Cholinergic deficits in the septal-hippocampal pathway of the SAM-P/8 senescence accelerated mouse. *Brain Res* **966**: 150–156.

Tribollet E, Bertrand D, Marguerat A, Raggenbass M (2004). Comparative distribution of nicotinic receptor subtypes during development, adulthood and aging: an autoradiographic study in the rat brain. *Neuroscience* **124**: 405–420.

Wang F, Nelson ME, Kuryatov A, Olale F, Cooper J, Keyser K *et al* (1998). Chronic nicotine treatment up-regulates human alpha3 beta2 but not alpha3 beta4 acetylcholine receptors stably transfected in human embryonic kidney cells. *J Biol Chem* **273**: 28721–28732.